A New Perspective in the Lewis Acid Catalyzed Ring Opening of Epoxides. Theoretical Study of Some Complexes of Methanol, Acetic Acid, Dimethyl Ether, Diethyl Ether, and Ethylene Oxide with Boron Trifluoride

Patricia Saenz,[‡] Raúl E. Cachau,[†,§] Gustavo Seoane,[‡] Martina Kieninger,[†] and Oscar N. Ventura*[,†]

Computational Chemical Physics Group, Detema, and Department of Organic Chemistry, Faculty of Chemistry, Universidad de la República (Udelar), CC1157, Avda. Gral. Flores 2124, 11800 Montevideo, Uruguay, and Advanced Biomedical Computing Center, National Cancer Institute-Frederick, SAIC-Frederick Inc., Frederick, Maryland 21702-1201

Received: March 4, 2006; In Final Form: May 15, 2006

Several 1:1, 1:2, and 2:2 complexes between BF_3 and CH_3OH (Met), CH_3COOH (AcA), $(CH_3)_2O$ (DME), $(CH_3CH_2)_2O$ (DEE), and $(CH_2)_2O$ (EOX) have been studied using ab initio (MP2) and density functional theory (DFT) (PBE, B3LYP) methods and the 6-311++G(3df,2pd) basis set. Geometrical structures and vibrational frequencies are reported, in most cases, for the first time. A detailed comparison of the vibrational frequencies for the O···BF_3 vibrational modes, as well as for the ν(OH) band in the methanol and acetic acid complexes with BF_3, is performed, and the theoretical frequency shifts are compared with the available experimental information. Thermochemical properties are calculated by employing counterpoise correction to alleviate the basis set superposition error. The DFT enthalpy of complexation of the 1:1 complexes results in the order of stability $(AcA)_2$ > AcA:BF_3 > DEE:BF_3 > DME:BF_3 > Met:BF_3 > EOX:BF_3 > $(Met)_2$; in contrast, MP2 shows the noticeable difference that the AcA:BF_3 complex is much less stable (similar to Met:BF_3). The order of stability shows that, even though acetic acid prefers dimerization to complexation with BF_3, the case is exactly the opposite for methanol. In both cases, the interaction of BF_3 with the dimer gives rise to very stable trimers. However, in contrast to the interaction of BF_3 with the methanol dimer being stronger than that with the monomer, the interaction of BF_3 with the acetic acid dimer is weaker than that with the monomer. The relative strength of the complexes, discussed in the context of BF_3-catalyzed ring opening of epoxides, suggests that the effect of the catalyst in a nonprotogenic solvent should be more properly ascribed to activation of the nucleophile instead of activation of the epoxide.

Introduction

Boron trifluoride is a highly toxic, colorless gas, used extensively as a catalyst in organic chemistry. It reacts readily with water, producing hydrogen fluoride and boric acid. Thus, although commercially available at high purity, it is more conveniently handled when dissolved in appropriate solvents. The most common formulation found in the organic chemistry laboratory is the diethyl ether solution, known as boron trifluoride diethyl etherate (btdee). It is a fuming liquid with a high boiling point (126 °C), suggesting a relatively strong interaction between the donor (diethyl ether) and the acceptor (BF_3). Other commercial presentations (for instance, from BASF) are the BF_3-CH_3COOH (btaa) and BF_3-CH_3OH (btm) complexes. The first is a viscous liquid, colorless to brown, with an even higher boiling point (140−148 °C), and the second is a clear, fuming liquid, with a flash point at 61 °C. Two different complexes between boron trifluoride and methanol have actually been identified: a 1:1 complex that associates through hydrogen bonding (btm) and a 1:2 complex (bt2m), when methanol is in excess. The same situation seems to hold for the complex with acetic acid.

btdee is currently used in many chemical reactions, such as the ring opening of epoxides. It is currently accepted that ring opening by an alcohol, for instance, is facilitated by the attachment of the BF_3 Lewis acid to the oxygen atom in the epoxide; one of the carbons is then attacked by the entering group.[1] The exact mechanism in nonprotonogenic solvents has not been thoroughly investigated however. In our own experiments on the epoxide ring opening of (1*R*,2*R*,3*R*,4*S*)-1,2-oxi-3,4-*O*-isopropyliden-5-chloro-5-cyclohexen-2,3-diol reported elsewhere,[2] we have found the counterintuitive result that BF_3-catalyzed ring opening in dichloromethane was achieved more easily by 3-chlorobenzoic acid than by 4-methoxybenzyl alcohol. In the quest of clues to explain this behavior, we came across the difficulty pointed out above about the lack of knowledge on the exact mechanism. One of the unknown aspects is the exact nature of the pre-reactive complexes involved. For instance, it is not known whether the Lewis acid is bound to the epoxide before the reaction starts or if it is incorporated along the reaction path. Neither is it known whether BF_3 binds to the nucleophiles, and if so, how. And finally, the reaction path is not known for hydrogen migration from the alcohol to the epoxide oxygen when no dissociation is possible and no Brønsted base is involved. Thus, we chose to perform an initial study on the complexes btm, bt2m, btdee, btaa, and bt2aa, as well as on the boron trifluoride dimethyl etherate (btdme) and the complex of BF_3 with ethylene oxide (bteox) to extract some

*Corresponding author. Telephone number: +5982 924 8396. Fax number: +5982 924 1906. E-mail: onv@fq.edu.uy.
[†] Computational Chemical Physics Group, Udelar.
[‡] Department of Organic Chemistry, Udelar.
[§] National Cancer Institute.

10.1021/jp061359y CCC: $33.50
Published on Web 09/19/2006

hints about the structure and relative stability of the pre-reactive complexes in more complicated situations.

The first in-depth study of the etherates is the work by Brown and Adams,[3] who derived enthalpies of formation for both btdme (−55.6 kJ/mol) and btdee (−45.6 kJ/mol) almost simultaneously with Laubengayer and Finlay,[4] who reported more precise enthalpies of formation for btdme (−58.1± 2.9 kJ/mol) and btdee (−52.25 ± 4.18 kJ/mol). They also found that the etherates were monomeric when dissolved in benzene and the charge transfer (as indicated by the contribution of the donor−acceptor bond to the total dipole moment) was small. An electron diffraction structure determination of btdme by Bauer, Finlay, and Laubengayer[5] immediately followed. They assumed local tetrahedral environments for B and C, obtaining a structure with tetrahedral valence angles for oxygen and a B−O distance of 1.52 ± 0.06 Å (later[6] corrected to 1.50 ± 0.06 Å). More recently, however, Iijima et al.[7] performed another electron diffraction study and concluded that the B−O distance is larger (1.75 ± 0.02 Å at 70 °C).

McLaughlin and Tamres[8] studied these compounds again some years later and proposed enthalpies of formation of −57.06 ± 0.84 kJ/mol for btdme and −49.87 ± 1.25 kJ/mol for btdee. In the meantime, Greenwood et al.[9] and Grimley and Holliday[10] have studied bteox and found a stable 1:1 complex below −80 °C. McLaughlin et al.[11] found that bteox prepared at −20 °C underwent a rapid and irreversible reaction when allowed to warm to room temperature, yielding a gummy polymer whose formation was accompanied by the considerable evolution of heat. Other cyclic ethers such as tetrahydrofuran and tetrahydropyran formed stable 1:1 adducts with BF_3 at room temperature. More recently, Maria and Gal[12] reported the enthalpies of formation at room temperature of the complexes of BF_3 with 75 nonprotonogenic solvents in dichloromethane. The $\Delta_f H°_{298.15}$ for the complexation of diethyl ether with BF_3 was measured in both CH_2Cl_2 and ϕ-NO_2, giving −78.77 ± 0.38 and −81.35 ± 0.38 kJ/mol, respectively. The first theoretical calculation of btdme seems to be the work of Jonas et al.,[13] who found a B−O distance of 1.680 Å at the MP2/TZ2P level, intermediate between the two available electron diffraction results. The enthalpy of formation of the complex was calculated as −72.3 kJ/mol, which agrees very well with the result of Maria and Gal[12] in dichloromethane just by chance, because the calculated value must be comparable to the gas-phase measure, about −57 kJ/mol according to McLaughlin and Tamres.[8] Results nearly identical to those of Jonas et al.[13] were published simultaneously by Rauk et al.,[14] who used the MP2 and MP3 methods with the 6-31G(d) basis set: optimum B−O distance of 1.696 Å and −71 kJ/mol for the enthalpy of complexation at 298 K. A comparison between the experimental and theoretical IR spectra of btdme was performed by Nxumalo and Ford.[15] Regretfully, their calculations were performed at the RHF/6-31G(d) level, which neglects all the effects of correlation energy. Another work performed at the Hartree−Fock level, although with a slightly larger 6-311G(d,p) basis set, is that of Ring et al.[16] superseded by the calculations of Roswell et al.[17] of btdme at the B3LYP/6-311+G(2d,p) level, obtaining an optimum B−O distance of 1.712 Å, somewhat intermediate between the experimental values and near the MP2 value. Finally, a paper by Fãrcaşiu et al.[18] reports a ^{13}C NMR study of btdee with the derivation of an enthalpy of activation for decomposition of the complex, in essential agreement with the enthalpy of formation in the gas phase derived in previous experiments.

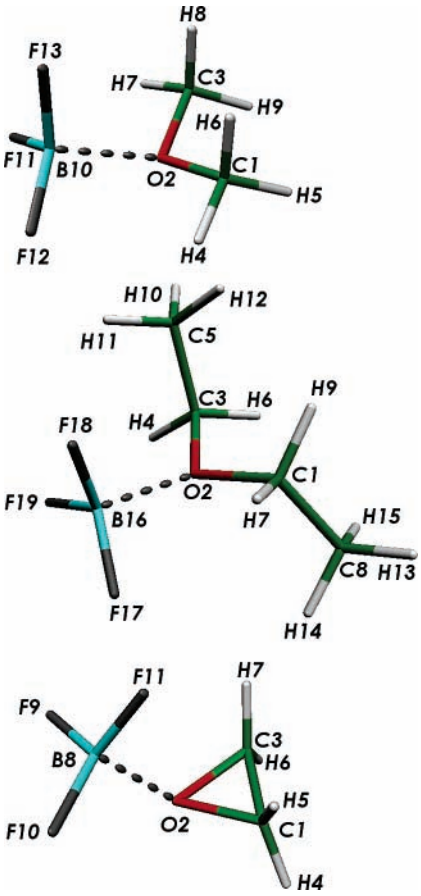

Figure 1. Structure of the complexes of BF_3 with dimethyl ether (btdme), diethyl ether (btee), and ethylene oxide (bteox). The numbering of the atoms helps in the identification of the geometrical parameters displayed in Tables 1−3.

Data are much less abundant for the other complexes, with some results present for btm, bt2m, btaa, and bt2aa. From the experimental point of view, most of the data are contained or referenced in the paper by Derouault et al.[19] A previous work by Taillandier et al.[20] reported a partial IR analysis of btm, bt2m, btaa, and bt2aa. No other information about the structure or spectra of these complexes seems to exist in the literature. From the theoretical point of view, the 1:1 btm geometry was optimized only at the RHF/6-31G(d) level by Rauk et al.,[14] and no calculation seems to be present on the structure of the 1:1 complex btaa. The bt2m complex was recently studied theoretically by Haubein et al.[21,22] at the B3LYP level, and no other calculation seems to be present in the literature. The experimental data[19,23] suggest that for the 2:1 bt2m complex and at larger relative concentrations of methanol to BF_3 there is dissociation into $CH_3OBF_3^-$ and $CH_3OH_2^+$, but this seems not to be the case for the 1:1 btm complex. No theoretical calculation for bt2aa seems to be present in the literature.

Our purpose in this work is to study the structure and energetics of the complexes of BF_3 with methanol, dimethyl ether, diethyl ether, acetic acid, and ethylene oxide. The main goals are to assess whether there is a significant difference in nucleophilicity between the uncomplexed nucleophiles and the BF_3 complexes and to discuss the relative stability of the complexes in the context of BF_3-catalyzed epoxide ring opening.

Methods

The 1:1 complexes of BF_3 and methanol, acetic acid, dimethyl ether, diethyl ether, and ethylene oxide, as well as the 2:1 and

TABLE 1: Experimental and Calculated Geometries of the 1:1 Complex of BF_3 with Dimethyl Ether (btdme)

	PBE[b]		B3LYP[b]		MP2[b]			
parameter[a]	small	large	small	large	small	large	exptl	other calculations
d(O2B10)	1.707	1.679	1.742	1.710	1.696	1.671	1.75 ± 0.02[c] 1.50 ± 0.06[d] 1.52 ± 0.06[e]	1.680,[f] 1.696,[g] 1.695,[h] 1.69,[i] 1.712[j]
d(O2C1)	1.431	1.430	1.442	1.442	1.449	1.439	1.45 ± 0.03[d]	1.442,[f] 1.425,[h] 1.446[j]
d(C1H4)	1.088	1.085	1.088	1.083	1.086	1.082		1.079[h]
d(C1H5)	1.093	1.089	1.093	1.088	1.091	1.086		1.079[h]
d(C1H6)	1.095	1.091	1.095	1.090	1.092	1.088		1.083[h]
d(B10F12)	1.353	1.350	1.355	1.354	1.364	1.354	1.43 ± 0.03[d] 1.41 ± 0.02[e]	1.354,[f] 1.342,[h] 1.347,[i] 1.355[j]
d(B10F13)	1.360	1.358	1.361	1.361	1.373	1.364	1.43 ± 0.03[d] 1.41 ± 0.02[e]	1.362,[f] 1.348,[h] 1.347,[i] 1.363[j]
d(H4F12)	2.343	2.357	2.369	2.383	2.358	2.367		
d(H6F13)	2.698	2.745	2.754	2.827	2.648	2.650		
θ(C1O2C3)	113.0	112.8	113.3	113.2	112.1	111.6		111.4,[f] 114.2,[h] 114.5,[i] 113.0[j]
θ(C1O2B10)	113.4	114.4	113.8	115.2	112.6	113.2		113.3,[f] 115.9,[h] 116.6,[i] 114.7[j]
θ(O2C1H4)	106.2	106.9	106.1	106.8	105.9	106.7		107.8[h]
θ(O2C1H5)	108.6	108.4	108.7	108.3	108.1	108.0		107.8[h]
θ(O2C1H6)	110.0	109.9	110.0	109.9	109.6	109.5		108.3[h]
θ(O2B10F12)	101.7	102.5	101.3	102.2	102.0	102.5		102.4,[f] 102.3,[h] 102.1[j]
θ(O2B10F13)	102.3	103.4	102.0	103.2	102.6	103.2		103.4,[f] 102.6,[h] 103.3[j]
θ(F12B10F13)	115.5	114.9	115.8	115.1	115.3	114.8		114.9,[f] 115.2,[h] 115.1[j]
φ(C3O2C1H4)	−179.1	−178.0	−178.8	−177.5	−179.2	−178.4		
φ(C3O2C1H5)	−60.0	−58.9	−59.7	−58.4	−60.1	−59.2		
φ(C3O2C1H6)	61.5	62.2	61.8	62.6	61.2	61.7		
φ(B10O2C1H4)	50.1	48.9	49.2	47.0	52.6	52.4		
φ(B10O2C1H5)	169.2	168.0	168.3	166.1	171.6	171.6		
φ(B10O2C1H6)	−69.3	−71.0	−70.2	−72.9	−67.0	−67.5		
φ(F13B10O2C1)	65.3	66.2	65.9	67.3	64.0	64.2		
φ(F12B10O2C1)	−54.5	−53.6	−53.9	−52.5	−55.7	−55.4		
φ(F13B10C1H6)	0.7	−0.4	0.7	−0.8	1.1	0.6		
φ(C1O2C3B10)	−130.8	−133.2	−132.0	−135.5	−128.3	−129.2	140 ± 8[c]	−133.7[g]

[a] Bond lengths in Å, bond and dihedral angles in degrees; numbering of the atoms as in Figure 1. [b] "Small" and "large" refer to the 6-31G(d) and 6-311++G(3df,2pd) calculations, respectively. [c] Most recent electron diffraction determination, ref 7. [d] Correction[5] of the electron diffraction analysis of ref 5. [e] Electron diffraction data, ref 5. [f] MP2/TZ2P, ref 13. [g] MP2/6-31G(d), ref 14. [h] RHF/6-31G(d,p), ref 15. [i] RHF/6-311G(d,p), ref 16. [j] B3LYP/6-311+G(2d,p), ref 17.

2:2 complexes of methanol and BF_3 have been studied at the ab initio[24] and density functional[25] levels. Second-order Møller−Plesset (MP2)[26] perturbation theory was used at the post-Hartree−Fock level, and both the Perdew−Burke−Erzenhoff (PBE)[27] and three-parameter adiabatically connected Becke−Lee−Yang−Parr (B3LYP)[28] methods were employed at the density functional level. The Pople basis sets 6-31G(d) and 6-311++G(3df,2pd)[24] were used to represent small and medium/large one-electron basis sets. Geometry optimization was performed on all the species considered until variation in the geometrical parameters was under 10^{-4} Å for all the Cartesian coordinates. Different relative positions of the monomers in the studied dimers and trimers were investigated using semiempirical methods. The resulting stable structures were used as initial points for the density functional theory (DFT) optimizations. Analytical second derivatives were calculated and used for determining the type of critical point on the PES and to calculate harmonic vibrational frequencies. Charge and electronic population analyses were performed using Weinhold's natural bond orbital (NBO) method.[29] Counterpoise calculations were performed for all dimers, trimers, and tetramers in the usual way.[30] All calculations were performed using Gaussian 03[31] in a multinode Itanium 2 server.

Results

Optimum geometries of the isolated reactants, as well as their harmonic vibrational frequencies, obtained at the levels of calculation employed in this paper can be obtained from the authors. Most of the complexes reported have been calculated before at a low level of theory or not at all. Therefore, we understood it to be convenient to show their detailed geometric structure explicitly. The discussion will be organized as follows: first, the geometrical structure and the vibrational spectra will be analyzed, followed by a discussion of the thermochemistry of these complexes and the influence on the results of the basis sets and the methods chosen for the calculations. Finally, a discussion of how these data have relevance in the study of Lewis acid catalyzed ring opening of epoxides will be presented.

Geometric Structure. We will describe first the interactions of BF_3 with the three nonprotonogenic species [$(CH_3)_2O$ (DME), $(CH_3CH_2)_2O$ (DEE), $(CH_2)_2O$ (EOX)], which follow similar patterns (see Figure 1 and Tables 1−3). BF_3 interacts with a lone pair on the oxygen atom, receiving electronic charge from the oxygen base and adopting a pyramidal structure due to the transfer of electronic density from the oxygen lone pairs to the vacant orbital in boron. The charge transfers between the two moieties in the complex, calculated using Weinhold's method,[29] are not identical but are similar in the three cases. Charge transfer does not show a large dependency on the basis set or method used and is around 0.20 ± 0.03 electrons. However, there is a marked difference in the detailed geometry of the three complexes. As shown in Tables1−3 and comparatively in Table 4, the B−O distance shortens by about 0.060 Å in passing from bteox to btdme to btdee; in contrast, the pyramidal disposition of the BOCC framework flattens from around 110° to around 150° (measuring this angle between the B−O line and the OCC plane). The reason for both effects should be found in the interaction between the fluorine atoms in BF_3 and the

TABLE 2: Calculated Geometries of the 1:1 Complex of BF_3 with Diethyl Ether (btdee)

	PBE[b]		B3LYP[b]		MP2[b]	
parameter[a]	small	large	small	large	small	large
d(O2C1)	1.448	1.444	1.461	1.457	1.464	1.450
d(O2C3)	1.444	1.443	1.457	1.456	1.460	1.450
d(O2B16)	1.668	1.646	1.695	1.669	1.664	1.642
d(C1H7)	1.092	1.088	1.091	1.086	1.090	1.085
d(C1H9)	1.094	1.091	1.093	1.089	1.092	1.089
d(C1C8)	1.510	1.506	1.517	1.513	1.512	1.509
d(C3H4)	1.090	1.087	1.893	1.085	1.088	1.085
d(C3H6)	1.095	1.091	1.095	1.089	1.093	1.089
d(C3C5)	1.513	1.508	1.521	1.515	1.514	1.511
d(C5H10)	1.095	1.092	1.096	1.091	1.094	1.089
d(C5H11)	1.092	1.089	1.092	1.087	1.089	1.085
d(C5H12)	1.095	1.091	1.095	1.090	1.093	1.088
d(C8H13)	1.095	1.091	1.096	1.091	1.094	1.089
d(C8H14)	1.092	1.090	1.092	1.088	1.090	1.087
d(C8H15)	1.095	1.091	1.095	1.090	1.093	1.088
d(B16F17)	1.359	1.356	1.361	1.360	1.369	1.359
d(B16F18)	1.364	1.361	1.366	1.364	1.376	1.366
d(B16F19)	1.358	1.355	1.360	1.359	1.369	1.359
θ(C1O2C3)	117.0	116.2	117.2	116.7	116.1	114.9
θ(C1O2B16)	115.7	116.7	116.1	117.4	114.6	115.5
θ(C3O2B16)	118.6	119.8	118.3	120.3	117.9	118.6
θ(O2C1H7)	106.6	105.7	106.6	105.7	106.6	105.7
θ(O2C1H9)	107.6	108.0	107.5	107.8	107.5	108.1
θ(O2C1C8)	109.7	110.6	109.8	110.7	108.7	109.7
θ(O2C3H4)	104.2	105.0	104.0	104.8	104.2	104.9
θ(O2C3H6)	106.5	106.3	106.5	106.3	105.9	106.0
θ(O2C3C5)	113.0	112.9	113.2	113.0	112.8	112.7
θ(C3C5H10)	109.1	108.8	109.0	108.7	108.8	108.5
θ(C3C5H11)	110.7	110.8	110.7	110.9	110.7	110.7
θ(C3C5H12)	111.9	112.2	111.9	112.1	111.7	111.8
θ(C1C8H13)	109.8	109.4	109.7	109.3	109.8	109.4
θ(C1C8H14)	109.7	110.3	109.8	110.4	109.4	110.0
θ(C1C8H15)	111.3	111.9	111.2	111.8	110.8	111.6
θ(O2B16F17)	101.9	102.7	101.8	102.6	101.8	102.5
θ(O2B16F18)	104.3	105.0	104.0	104.8	104.8	104.9
θ(O2B16F19)	102.4	103.0	102.1	102.9	102.4	102.8
ϕ(C3O2C1H7)	126.6	148.2	124.0	146.2	125.2	149.7
ϕ(C3O2C1H9)	10.7	32.7	8.0	30.6	9.0	33.6
ϕ(C3O2C1C8)	−111.7	−90.8	−114.2	−92.7	−113.1	−89.7
ϕ(B16O2C1H7)	−20.7	−2.0	−23.9	−7.4	−17.7	−6.0
ϕ(B16O2C1H9)	−136.6	−117.5	−139.8	−123.0	−134.0	−110.1
ϕ(B16O2C1C8)	101.1	119.0	98.0	113.7	103.9	126.6
ϕ(C1O2C3H4)	162.9	156.9	163.7	156.5	161.6	156.8
ϕ(C1O2C3H6)	48.0	42.0	48.8	41.5	46.6	41.5
ϕ(C1O2C3C5)	−75.7	−81.4	−75.0	−81.9	−76.8	−81.5
ϕ(B16O2C3H4)	−50.8	−53.9	−49.2	−50.7	−56.7	−60.6
ϕ(B16O2C3H6)	−165.6	−168.8	−164.1	−165.7	−171.7	−176.0
ϕ(B16O2C3C5)	70.6	67.7	72.1	70.9	64.9	61.0
ϕ(C1O2B16F17)	−53.1	−56.7	−50.8	−53.4	−57.6	−61.5
ϕ(C1O2B16F18)	66.1	62.6	68.6	66.0	61.5	57.7
ϕ(C1O2B16F19)	−173.7	−177.2	−171.3	−173.8	−178.4	177.9
ϕ(C3O2B16F17)	160.1	154.2	161.8	154.0	160.1	156.2
ϕ(C3O2B16F18)	−80.6	−86.5	−78.9	−86.6	−80.7	−84.6
ϕ(C3O2B16F19)	39.6	33.8	41.3	33.6	39.4	35.6
ϕ(O2C1C8H13)	−178.6	−179.3	−178.7	−179.2	−179.0	−179.2
ϕ(O2C1C8H14)	−59.1	−59.9	−59.1	−59.9	−59.3	−59.8
ϕ(O2C1C8H15)	61.5	61.3	61.5	61.4	61.0	61.2
ϕ(O2C3C5H10)	−179.2	179.9	−178.2	179.8	178.8	178.1
ϕ(O2C3C5H11)	−59.5	−60.8	−58.5	−59.9	−61.6	−62.5
ϕ(O2C3C5H12)	61.6	60.7	62.6	61.1	59.5	58.9
ϕ(C1O2C3B16)	−146.3	−149.2	−147.1	−152.8	−141.7	−142.5

[a] Bond lengths in Å, bond and dihedral angles in degrees; numbering of the atoms as in Figure 1. [b] "Small" and "large" refer to the 6-31G(d) and 6-311++G(3df,2pd) calculations, respectively.

TABLE 3: Calculated Geometries of the 1:1 Complex of BF_3 with Ethylene Oxide (bteox)

	PBE[b]		B3LYP[b]		MP2[b]	
parameter[a]	small	large	small	large	small	large
d(C1O2)	1.444	1.441	1.457	1.453	1.467	1.455
d(C1C3)	1.462	1.458	1.468	1.462	1.465	1.461
d(C1H4)	1.085	1.082	1.086	1.080	1.084	1.079
d(C1H5)	1.085	1.082	1.085	1.003	1.083	1.079
d(B8O2)	1.730	1.706	1.770	1.744	1.728	1.705
d(B8F9)	1.346	1.343	1.347	1.346	1.357	1.347
d(B8F11)	1.364	1.360	1.365	1.362	1.375	1.364
θ(O2C1H4)	112.6	112.6	112.7	112.6	112.2	112.1
θ(O2C1H5)	113.5	113.6	113.6	113.7	113.4	113.3
θ(C3C1H4)	120.3	120.2	120.4	120.3	120.2	119.9
θ(C3C1H5)	118.6	118.6	118.8	118.8	118.8	118.5
θ(H4C1H5)	117.5	117.5	117.2	117.3	117.6	118.1
θ(C1O2B8)	117.5	118.8	117.9	119.7	116.5	117.5
θ(F9B8O2)	101.0	101.4	100.6	101.0	101.0	101.1
θ(F11B8O2)	101.9	103.2	101.4	102.8	102.4	103.3
ϕ(H4C1O2B8)	139.3	138.3	139.1	137.7	140.3	139.6
ϕ(H5C1O2B8)	2.7	1.6	2.7	1.3	4.2	3.0
ϕ(C1O2B8F9)	154.1	154.7	154.1	154.9	153.3	153.9
ϕ(C1O2B8F10)	−84.6	−84.2	−84.7	−84.1	−85.4	−85.0
ϕ(C1O2B8F11)	34.8	35.3	34.7	35.4	33.9	34.5
ϕ(C1O2C3B8)	−107.8	−108.8	−107.9	−109.4	−106.7	−107.6

[a] Bond lengths in Å, bond and dihedral angles in degrees; numbering of the atoms as in Figure 1. [b] "Small" and "large" refer to the 6-31G(d) and 6-311++G(3df,2pd) calculations, respectively.

hydrogen atoms in the ether or epoxide. As is shown in Figure 1, one of the F atoms in the bteox complex exhibits a relatively strong interaction with two hydrogens of ethylene oxide (both F−H distances are 2.431 Å at the PBE/6-311++G(df,2pd) level) on the same face of the epoxide; there is no interaction between the other F atoms and the H atoms on the opposite face. Therefore, pyramidalization is the largest effect found in the three complexes. For btdme, there is a pair of additional F−H interactions, both of them with a smaller distance (2.357 Å) calculated at the same level as before. These interactions are on the opposite face of the OCC plane with respect to the F13 interaction with H8 and H6; this tends to flatten the pyramidalization angle. Finally, the interaction in btdee is more complex, with three F−H short distances, as depicted in Figure 2. Again, these are attractive interactions and tend to reduce the B−O distance as the pyramidalization angle approaches planarity. An indirect support to this analysis can be found in the RHF/6-31G(d) results obtained by Rauk et al.[14] Besides studying btdme, they also investigated the complexes of BF_3 with oxetane, tetrahydrofuran and 7-oxanorbornene, obtaining the same variation in the B−O distance as that reported here. Moreover, Corey et al.[32] proved that BF_3 complexes of formyl compounds exhibit a conformational restriction arising from the interaction between one of the fluorine atoms and the formyl hydrogen, a CH···F hydrogen bond. Clearly, the formyl hydrogen is more polar than those in our complexes, but the principle for the stabilization is the same. Additionally, this stabilization is supported by the experimental and theoretical data of Güizado-Rodríguez et al.,[33] who studied the BH_3 and BF_3 adducts of 1,3-dimethyl-1,3-diazolidine and found evidence of weak proton−fluoride interactions. Thus, it is reasonable to think that the F···H attractive interactions are responsible for the structural differences among the complexes.

btdme is probably the best known of these three complexes. It has been studied experimentally in cryogenic matrixes,[34−39] using electron diffraction methods,[5,6,40] by IR and Raman spectroscopy in the gas, liquid, and solid phases[41−43], and theoretically.[13−17,37,44] The calculated structures of btdme obtained by other authors at less precise levels do agree with the ones we determined. In particular, looking at the other published MP2 and B3LYP calculations together with our calculations, one appreciates that the increase in the basis set produces a notorious shortening of the B−O distance. Therefore, previous

TABLE 4: Compendium of Experimental and Calculated Donor−Acceptor Bond Lengths and Pyramidalization Angles for the 1:1 Complexes of BF_3 with DME, DEE, and EOX

		Me_2O-BF_3		Et_2O-BF_3		$c\text{-}(CH_2)_2O-BF_3$	
methods		d(B−O)/Å	ϕ/deg	d(B−O)/Å	ϕ/deg	d(B−O)/Å	ϕ/deg
exptl	ED	1.75 ± 0.02[a]					
	ED	1.52 ± 0.06[b]					
	ED	1.50 ± 0.06[c]					
MP2	6-31G(d)	1.696[d]					
MP2	TZ2P	1.680[e]					
B3LYP	6-311+G(2d,p)	1.712[f]					
PBE	6-31G(d)	1.707	−130.8	1.668	−146.3	1.730	−107.8
	6-311++G(3df,2pd)	1.679	−133.2	1.646	−149.2	1.706	−108.8
B3LYP	6-31G(d)	1.742	−132.0	1.695	−147.1	1.770	−107.9
	6-311++G(3df,2pd)	1.710	−135.5	1.669	−152.8	1.744	−109.4
MP2	6-31G(d)	1.696	−128.3	1.664	−141.7	1.728	−106.7
	6-311++G(3df,2pd)	1.671	−129.2	1.642	−142.5	1.705	−107.6

[a] Reference 7. [b] Reference 6. [c] Reference 5. [d] Reference 14. [e] Reference 13. [f] Reference 17.

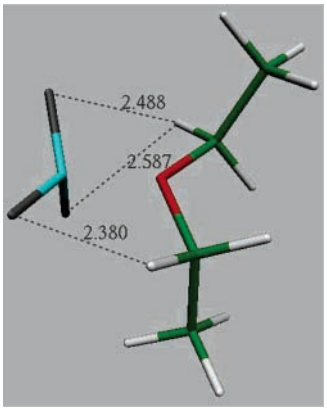

Figure 2. Schematics of the F−H attractive interactions in btdee. The values shown were obtained at the PBE/6-311++G(3df,2pd) level. See also Table 2.

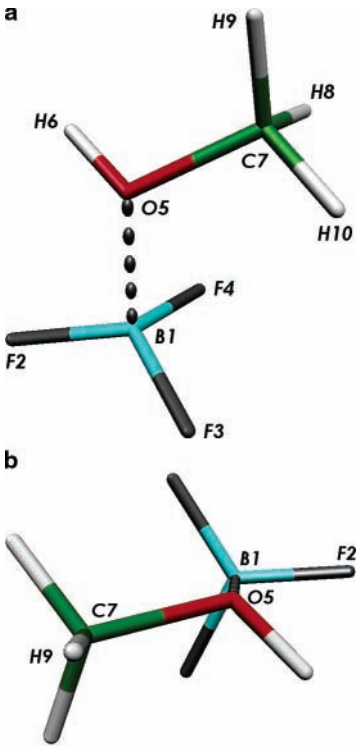

Figure 3. Structure of the 1:1 methanol−BF_3 complex (btm), showing the numbering of the atoms: (a) lateral view; (b) top view, showing the quasi-planarity of the F2−B1−O5−C7−H9 bond structure.

claims on the agreement between the theoretical and experimental B−O distances are groundless. In fact, there is a very large difference of 0.08 Å between our best results, presently the larger ones published, and the most recent experimental result, although the calculated pyramidalization angle is more in agreement with the experimental (140 ± 8°) result. Several reasons may account for the deficiency. First, theoretical calculations afford minimum equilibrium distances, not the vibrationally averaged experimental ones, which make an appreciable difference when dealing with nonbonded interactions.[45] Second, the experimental results do depend on the temperature at which the experiments are performed (the experimental distance determined at 291 K is 0.02 Å shorter than that determined at 345 K), and the theoretical results correspond to 0 K. Third, the experimental intermolecular parameters were obtained by assuming local C_{3v} symmetry of the BF_3 and CH_3 groups and there is an appreciable difference in the length of the B−F and C−H bonds in the optimum structures. And finally, one should not disregard that there are large discrepancies between the experimental determinations themselves. All in all, one could expect that the results shown here are fairly precise nonvibrationally averaged equilibrium geometries. Because they are the ones obtained at the largest level up to now (and for btdee and bteox seem to be the only ones available), they should be good starting points for further studies.

Complexes of BF_3 with methanol and with acetic acid present different challenges than those of BF_3 with the ethers. In the first case, the study by Derouault et al.[19] showed the presence of two complexes, btm and bt2m, depending on the relative concentrations of methanol and boron trifluoride. Their experimental results for the 1:1 btm complex could be best explained by assuming that boron links to oxygen in a tetrahedral disposition similar to that found in the etherates. Our own theoretical results show exactly this structure, with an approximate CBO symmetry plane that also contains one C−H and one B−F bond (see Figure 3b, where one can see that the atoms F2−B1−O5−C7−H9 are almost coplanar). Looking along the B−O axis, one sees that the O−H bond has a transoid disposition with respect to one B−F bond. This configuration allows for relatively small distances between F2 and F4 and the hydroxyl H6 on one side, and between F4 and H8 and between F3 and H10 on the other, therefore maximizing attractions (see Table 5). Moreover, from Tables 4 and 5, one can see that both the B1−O5 distance and the angle of pyramidalization are similar to those of btdme. No recent

TABLE 5: Geometries of the 1:1 btm Complex

	PBE[b]		B3LYP[b]		MP2[b]	
parameter[a]	small	large	small	large	small	large
d(O5C7)	1.437	1.437	1.448	1.449	1.454	1.445
d(O5H6)	0.970	0.962	0.972	0.964	0.977	0.964
d(C7H9)	1.092	1.088	1.092	1.087	1.089	1.084
d(C7H8)	1.092	1.089	1.092	1.087	1.089	1.085
d(C7H10)	1.089	1.086	1.089	1.084	1.086	1.082
d(B1O5)	1.716	1.689	1.756	1.727	1.712	1.687
d(B1F2)	1.353	1.350	1.354	1.353	1.363	1.352
d(B1F3)	1.349	1.346	1.350	1.349	1.360	1.350
d(B1F4)	1.359	1.356	1.360	1.358	1.370	1.360
d(F2H6)	2.412	2.427	2.429	2.450	2.440	2.441
d(F4H6)	2.693	2.685	2.730	2.735	2.684	2.671
d(F4H8)	2.549	2.608	2.579	2.672	2.550	2.572
d(F3H10)	2.636	2.628	2.703	2.689	2.598	2.594
θ(C7O5H6)	110.7	111.2	110.6	111.3	110.3	110.6
θ(H9C7O5)	109.0	108.8	109.0	108.7	108.4	108.5
θ(H8C7O5)	110.6	110.4	110.6	110.3	110.3	110.1
θ(H10C7O5)	105.3	106.0	105.2	105.9	104.9	105.6
θ(B1O5C7)	115.3	116.8	115.7	117.8	114.5	115.7
θ(B1O5H6)	107.1	108.1	106.9	108.7	107.1	108.1
θ(F2B1O5)	99.7	100.4	99.1	100.0	100.0	100.6
θ(F3B1O5)	101.9	102.4	101.5	102.0	101.9	102.0
θ(F4B1O5)	102.6	103.5	102.1	103.2	102.7	103.3
ϕ(H6O5C7H9)	63.0	59.0	62.1	57.9	64.2	59.9
ϕ(H6O5C7H8)	−60.1	−63.5	−60.8	−64.5	−58.6	−62.5
ϕ(H6O5C7H10)	−178.9	177.3	−179.6	176.2	−177.5	178.3
ϕ(B1O5C7H9)	−175.3	−176.3	−176.1	−175.7	−174.9	−176.8
ϕ(B1O5C7H8)	61.7	61.2	61.0	61.9	62.3	60.8
ϕ(B1O5C7H10)	−57.1	−58.0	−57.8	−57.4	−56.6	−58.4
ϕ(B1O5H6C7)	−126.5	−129.5	−126.8	−131.3	−125.2	−127.6
ϕ(F2B1O5H6)	−44.0	−45.6	−42.7	−43.7	−46.5	−47.3
ϕ(F2B1O5C7)	−167.7	−171.8	−166.4	−171.4	−169.1	−172.0
ϕ(F3B1O5H6)	−165.0	−166.5	−163.6	−164.5	−167.6	−168.4
ϕ(F3B1O5C7)	71.3	67.2	72.6	67.8	69.8	67.0
ϕ(F4B1O5H6)	75.0	73.6	76.4	75.5	72.6	72.0
ϕ(F4B1O5C7)	−48.7	−52.7	−47.4	−52.1	−50.0	−52.6

[a] Bond lengths in Å, bond and dihedral angles in degrees; numbering of the atoms as in Figure 3. [b] "Small" and "large" refer to the 6-31G(d) and 6-311++G(3df,2pd) calculations, respectively.

theoretical study on btm other than that of Rauk et al.[14] seems to be available in the literature, and this one is at the very low HF/6-31G(d) level superseded by the calculations reported in this paper. More information about the structure can be obtained by comparison of the calculated vibrational frequencies with the experimental IR spectrum, which we will do in the next section.

The pioneering work of Diehl and Ogg[46] and Paasivirta and Brownstein[47] (employing NMR techniques) and of Taillandier et al.[20] (using IR spectroscopy) showed the existence of the 2:1 complex bt2m between methanol and boron trifluoride. The IR spectra of bt2m and deuterated analogues allowed Taillandier, Tochon, and Taillandier[20] to propose that the complex must have an open structure where a second methanol molecule is hydrogen-bonded to btm. Our calculations agree with this same conclusion, as can be seen in Table 6 and Figure 4. The second methanol molecule binds through a hydrogen bond to the first methanol molecule already present in the btm complex. However, this hydrogen bond is not the only stabilizing factor. In fact, one can identify a network of attractive interactions between the hydroxylic protons and fluorine, as well as between the methyl groups and the fluorine atoms. This network can be appreciated in the distances shown in Table 6, but it is perhaps more clear to have a graphic depiction, as in Figure 4b, where the PBE/6-311++G(3df,2pd) results are shown. Comparing the distances in the btm substructure within bt2m with those in btm itself, one sees that BF_3 is now more tightly bound (the B−O distance suffered a contraction of 0.09Å and the F2H6 and F4H6 distances are correspondingly shorter). The second methanol molecule has a very short hydrogen bond (H6O11 distance of about 1.6 Å), also suggested on the basis of experimental evidence by Derouault et al,[19] and a secondary stabilizing interaction between H16 and F4, which shows the smallest of all the HF distances in the complex. Finally, a minor stabilization effect is also afforded by the interaction between F2 and the methyl group of the second methanol, as shown by the distance between F2 and H15, similar to that between F3 and H10. As said before, the only other previous study on this complex was performed by Haubein et al.[21] at the B3LYP/6-31G(d,p) level. They also found the short O···HO hydrogen bond and the F··· ·HO interaction we discussed above. The results of their geometry optimization are consistent with the ones obtained in this paper, which were obtained at a better theoretical level.

The structure of the methanol dimer substructure in bt2m can be compared to that of the methanol dimer itself, for which there are a number of theoretical[48−54] and experimental[48,55−63] results. The corresponding geometrical parameters determined at the levels of theory employed in this paper are included in Table 6 to facilitate the comparison. The similarities and differences between the structures can be appreciated visually in Figure 4c. In summary, the presence of BF_3 induces a much shorter hydrogen bond between both methanol subunits, an increased OH bond length in the proton-donor methanol molecule, and a propensity toward formation of a (CH_3O^-:BF_3)($CH_3OH_2^+$) ion pair. This last assertion is substantiated by the marked increase in the point charge at H8, as well as the increase in the charge transfer between the subunits, to the point that the charge in the (CH_3O^-:BF_3) group in btm is about 0.60 electrons.

According to Derouault et al.,[19] both the 1:1 btm and 2:1 bt2m complexes autoassociate through a dipole−dipole interaction of the OBF_3 groups, but where btm complexes associate by hydrogen bonding, bt2m does not seem to do so. This may be understood on the basis of the structures in Figures 2 and 3. Although btm has a relatively free hydroxyl hydrogen that can participate in hydrogen bonds (as it does in forming bt2m), the situation in the 2:1 complex is less favorable. In fact, the hydroxyl H of the first methanol molecule is already involved in a hydrogen bond with the second methanol molecule, whereas the hydroxyl H of the latter is quite strongly bound by the interaction with F4. The six-membered B1−O5−H6−O11−H16−F4 structure is favorably arranged to help the H16−F4 interaction, and it is probably unfavorable to disrupt it to accommodate an additional methanol molecule. The case of the 1:1 complex is different. We saw already how it can interact with a second methanol molecule in bt2m. We tried then to investigate the interaction of two btm molecules in the tetramer.

Derouault et al.[19] mentioned two possible association schemes, one involving hydrogen bonding between the hydroxyl group of the two btm molecules and the other involving an interaction of the hydroxyl group in one btm molecule and a fluorine atom in the second one. On the basis of the experiments with deuterated species, they favored OH−OH hydrogen-bonded species as the preferred one for association. We tried both initial structures but were unable to obtain different minima. All calculations converged finally to an antiparallel dimer shown in Figure 5, which exhibits two very strong hydrogen bonds between a fluorine atom in one of the btm molecules and the hydroxyl H of the other btm molecule. The geometric structures of this complex obtained at the different levels of theory are shown in Table 7. Clearly, it is not possible to ensure that this

TABLE 6: Geometries of the 2:1 bt2m Complex

	Met_2-BF_3						Met_2					
	PBE[b]		B3LYP[b]		MP2[b]		PBE[b]		B3LYP[b]		MP2[b]	
parameter[a]	small	large	small	large	small	large	small	large	small	large	small	large
d(O5C7)	1.436	1.433	1.448	1.446	1.453	1.441	1.403	1.403	1.413		1.420	1.413
d(O5H6)	1.013	1.006	1.012	1.003	1.013	1.004	0.975	0.966	0.977		0.977	0.967
d(C7H9)	1.091	1.088	1.091	1.086	1.089	1.084	1.102	1.097	1.103		1.099	1.092
d(C7H8)	1.094	1.090	1.094	1.088	1.091	1.087	1.103	1.097	1.102		1.098	1.092
d(C7H10)	1.088	1.086	1.088	1.084	1.086	1.082	1.095	1.091	1.095		1.091	1.086
d(B1O5)	1.616	1.602	1.636	1.623	1.621	1.602						
d(B1F2)	1.362	1.360	1.364	1.364	1.373	1.364						
d(B1F3)	1.354	1.352	1.357	1.357	1.365	1.355						
d(B1F4)	1.394	1.385	1.396	1.387	1.401	1.388						
d(O11C12)	1.427	1.425	1.439	1.437	1.444	1.434	1.420	1.416	1.431		1.436	1.426
d(O11H16)	0.975	0.964	0.977	0.966	0.978	0.966	0.966	0.958	0.970		0.972	0.959
d(C12H15)	1.095	1.092	1.095	1.090	1.091	1.088	1.097	1.094	1.097		1.094	1.089
d(C12H13)	1.092	1.088	1.092	1.087	1.089	1.084	1.092	1.088	1.092		1.089	1.085
d(C12H14)	1.095	1.091	1.096	1.090	1.093	1.087	1.097	1.094	1.098		1.094	1.089
d(H16F4)	1.944	2.181	1.970	2.272	2.037	2.185						
d(O11H6)	1.606	1.588	1.640	1.630	1.644	1.589	1.868	1.892	1.898		1.912	1.882
d(F2H6)	2.549	2.510	2.572	2.541	2.537	2.490						
d(F4H6)	2.412	2.424	2.433	2.457	2.439	2.422						
d(F4H8)	2.698	2.714	2.748	2.787	2.620	2.621						
d(F3H10)	2.457	2.508	2.480	2.535	2.492	2.530						
d(F2H15)	2.510	2.714	2.525	2.832	2.495	2.608						
θ(C7O5H6)	109.9	110.7	110.0	110.9	109.2	109.7	107.9	108.9	108.1		107.3	107.9
θ(H9C7O5)	108.3	108.3	108.2	108.1	107.8	108.0	113.0	112.4	112.9		112.5	112.1
θ(H8C7O5)	110.4	110.5	110.2	110.3	109.9	110.1	112.9	112.4	112.8		112.4	112.1
θ(H10C7O5)	106.7	107.1	106.5	106.9	106.2	106.8	107.6	107.7	107.4		107.0	107.4
θ(B1O5C7)	115.5	116.7	116.1	117.7	114.4	115.5						
θ(B1O5H6)	103.8	103.8	104.3	104.8	103.7	103.1						
θ(F2B1O5)	103.3	103.3	103.1	103.2	103.2	103.1						
θ(F3B1O5)	105.5	106.0	105.2	105.6	105.2	105.8						
θ(F4B1O5)	103.6	104.2	103.4	104.1	103.8	104.1						
θ(C12O11H16)	108.0	109.0	107.9	109.2	107.6	108.5	107.7	109.0	107.7		107.4	108.6
θ(H15C12O11)	111.2	111.1	111.1	110.9	110.8	110.7	111.8	111.9	111.7		111.5	111.6
θ(H14C12O11)	110.5	110.5	110.4	110.4	110.1	110.3	111.7	111.5	111.6		111.3	111.2
θ(H13C12O11)		107.0					106.6	106.9	106.4		106.0	106.4
θ(H16F4B1)	103.6	100.3	104.0	100.7	102.8	99.8						
θ(O11H16F4)	135.2	126.1	135.5	124.4	132.3	125.6						
θ(O11H6O5)	158.0	162.4	157.7	162.6	158.5	162.6	159.4	174.3	158.0		160.4	169.3
θ(H16O11H6)	91.6	96.0	91.1	96.8	92.9	96.4	98.8	109.9	96.4		101.4	119.7
ϕ(H6O5C7H9)	62.7	60.9	62.1	59.5	61.1	60.1	60.1	61.1	60.2		59.9	59.6
ϕ(H6O5C7H8)	−58.7	−60.4	−59.3	−61.7	−60.3	−61.1	−62.6	−61.4	−62.4		−62.6	−62.7
ϕ(H6O5C7H10)	−178.2	179.9	−178.8	178.4	−179.9	179.1	178.8	179.9	178.9		178.7	178.5
ϕ(B1O5C7H9)	179.8	179.4	−179.9	−179.9	176.8	176.1						
ϕ(B1O5C7H8)	58.3	58.1	58.7	58.9	55.4	54.9						
ϕ(B1O5C7H10)	−61.2	−61.7	−60.8	−61.0	−64.2	−64.8						
ϕ(F2B1O5H6)	−68.7	−66.0	−69.0	−66.1	−66.6	−64.9						
ϕ(F2B1O5C7)	170.9	171.9	169.9	170.2	174.6	175.4						
ϕ(F3B1O5H6)	168.4	171.5	168.3	171.6	170.6	172.5						
ϕ(F3B1O5C7)	48.0	49.4	47.1	47.9	51.8	52.7						
ϕ(F4B1O5H6)	48.6	51.3	48.5	51.3	50.8	52.3						
ϕ(F4B1O5C7)	−71.8	−70.8	−72.7	−72.4	−68.0	−67.4						
ϕ(H16O11C12H15)	56.8	59.6	57.1	60.2	57.7	59.4	65.8	60.6	66.4		64.8	58.5
ϕ(H16O11C12H14)	−65.6	−62.7	−65.2	−62.1	−64.7	−62.9	−57.6	−62.2	−56.9		−58.6	−64.3
ϕ(H16O11C12H13)	176.4	179.0	176.7	179.5	177.2	178.7	−175.8	179.8	−175.1		−176.8	177.0
ϕ(H16F4B1O5)	−47.1	−50.2	−46.7	−49.4	−48.8	−51.3						
ϕ(O11H16F4B1)	26.0	32.2	24.6	30.7	26.7	32.4						
ϕ(O11H6O5B1)	−21.4	−17.2	−20.4	−17.5	−22.6	−17.2						
ϕ(O16O11H6O5)	−7.0	−9.6	−8.7	−10.2	−6.8	−10.4	−73.4	−75.7	−67.4		−84.0	−134.9
ϕ(C12O11H6O5)	103.3	105.2	101.3	105.6	103.5	103.5	36.3	46.5	41.8		25.4	−11.3
ϕ(C12O11H16F4)	−109.8	−120.0	−108.2	−120.3	−110.1	−118.3						
ϕ(H16F4B1O5)	−47.1	−50.2	−46.7	−49.4	−48.8	−51.3						

[a] Bond lengths in Å, bond and dihedral angles in degrees; numbering of the atoms as in Figure 4. [b] "Small" and "large" refer to the 6-31G(d) and 6-311++G(3df,2pd) calculations, respectively.

structure will be present in the liquid 1:1 mixture. Gas-phase calculations produce a cyclic structure with preference given to the open-chain ones, but this may be due only to the lack of additional molecules in the model calculations. The structure of the btm dimer, however, is similar to that of the acetic acid dimer, studied among others by Chocholousova, Vacek, and Hobza,[64] who performed quantum chemical and molecular dynamics calculations on the dimer under different conditions (gas phase, microhydrated, diluted solution, and concentrated acid). They found that the dimer is not stable when water is added to the mixture. However, the dimer is stable in the gas phase and in chloroform solution, as well as in the crystal.[65] In

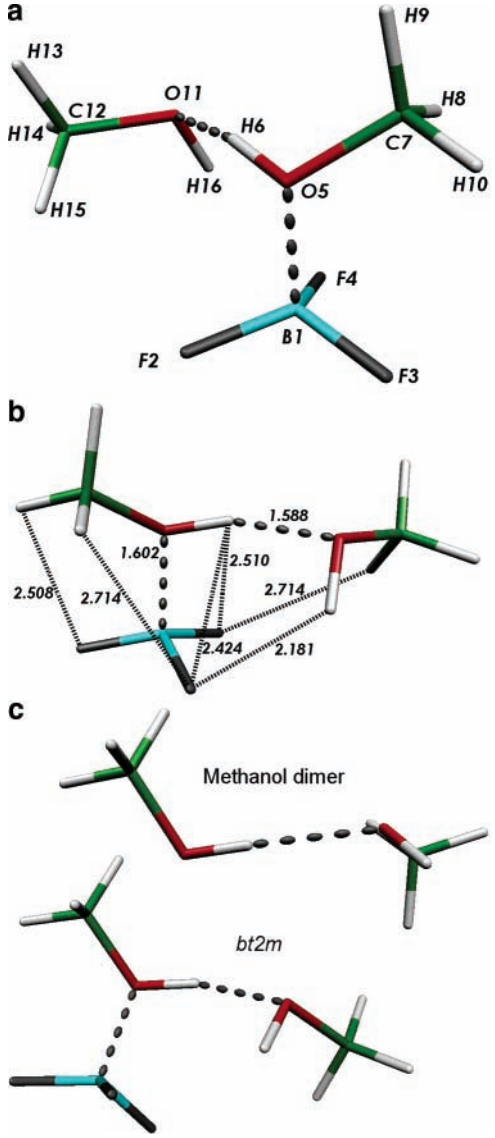

Figure 4. Structure of the 2:1 methanol−BF_3 complex (bt2m): (a) numbering of the atoms; (b) network of attractive interactions showing the distances calculated at the PBE/6-311++G(3df,2pd) level; (c) comparison of the structures of the methanol dimer and bt2m.

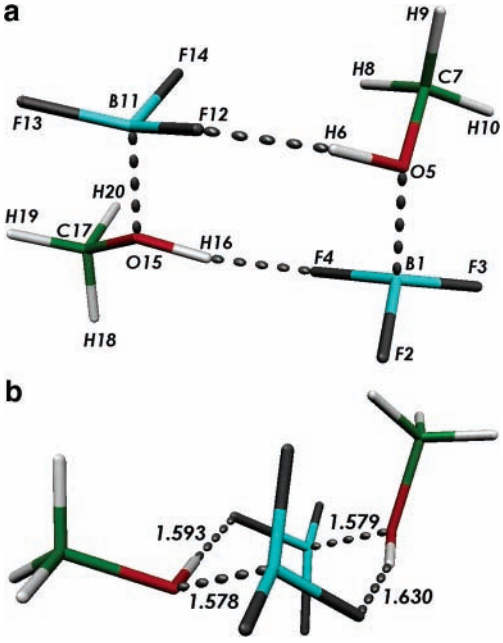

Figure 5. Structure of the $(CH_3OH:BF_3)_2$ tetramer, $(btm)_2$: (a) numbering of the atoms; (b) attractive interactions showing the distances calculated at the PBE/6-311++G(3df,2pd) level.

our case, there is no water present and the situation would probably be similar to that of neat acetic acid, for which Chocholousova et al.[64] propose the formation of chain structures, in agreement with a previous Raman spectral study,[66] which we will discuss later.

A perusal of the B−O distances in the cyclic dimer and the comparison with both btm and bt2m shows that the BF_3 moiety is now more tightly bound to the respective methanol molecule with which it forms the btm substructure. Looking, for instance, at the MP2/6-311++G(3df,2pd) results, one sees that the B−O length in the sequence btm, bt2m, and $(btm)_2$ varies from 1.687 to 1.602 to 1.580 Å (for both B−O bonds). Two hydrogen bonds are clearly identified between H16 and F4 and between F12 and H6, both because of the short F···H distances and because of the elongation of the C−F bond. For instance, all the calculations show a difference of about 0.07 Å between the hydrogen-bonded and non-hydrogen-bonded fluorine atoms. The cyclic dimer, however, is not symmetric. The essential difference can be seen in the F···HO bonds, one of which is longer (1.635 Å) than the other (1.597 Å) at all levels of calculation. This may be another indication that the cyclic dimer could be open to form chains in the neat btm liquid. At any rate, our results point toward F···HO bonds instead of toward the HO···HO bonds favored by Derouault et al.[19] Clearly, more research is needed to solve this problem.

Table 8contains the geometries of the btaa complex obtained at different levels of theory. Figure 6shows the numbering scheme employed for this complex. btaa is of course different from the other complexes we have studied up to now. The presence of the carboxylic oxygen simultaneously with the OH group anchors firmly in place the BF_3 moiety through the B−O dative bond and the F···HO hydrogen bond. Comparing the F···H distances, one sees that it is shorter in btaa (with some qualification to be discussed later) than in $(btm)_2$ and bt2m. The lengthening of the B−F bond, however, is comparable to that in the other complexes. Although there seems to be no experimental information or theoretical calculation on the geometry of this complex, there is abundant information on the 1:1 complexes of BF_3 with aldehydes and ketones. The experimental and theoretical studies done up to the beginning of the 1990s are well reviewed in the paper by Branchadell and Oliva.[67] Of particular interest is the study by Reetz et al.,[68] who performed an X-ray determination of the structure of the benzaldehyde−BF_3 complex. Branchadell and Oliva[67] performed MP2/6-31G(d)//RHF/6-31G(d) calculations on the formaldehyde−BF_3 adduct. Not surprisingly, the agreement with the experimental structure was only qualitative, although they were able to explain the general geometry of these complexes on the basis of an orbital interaction analysis. Gung and Wolf[69] performed almost simultaneously an MP2/6-31G(d)//RHF/3-21G calculation of the complexes of acetaldehyde, benzaldehyde, and acetone with BF_3. The results allowed them to propose the existence of an attractive interaction between the fluorine atoms in BF_3 and the hydrogen atoms in the methyl groups of acetaldehyde and acetone. Another landmark calculation was done by Jonas et al.,[13] who optimized the structure of the benzaldehyde−BF_3 complex at the MP2/6-31G(d) level. They found a general geometry in agreement with experiment and previous calculations but a B−O distance of 1.734 Å, significantly larger than the experimental 1.591 Å obtained by Reetz

TABLE 7: Geometries of the $(btm)_2$ Dimer

	PBE[b]		B3LYP[b]		MP2[b]			PBE[b]		B3LYP[b]		MP2[b]	
parameter[a]	small	large	small	large	small	large	parameter[a]	small	large	small	large	small	large
d(O5C7)	1.444	1.442	1.457	1.456	1.460	1.449	θ(B11O15H16)	108.7	110.3	108.8	110.9	107.8	109.1
d(O5H6)	0.992	0.985	0.993	0.985	0.994	0.984	θ(B11O15C17)	115.5	117.0	116.1	118.0	114.7	115.8
d(C7H9)	1.088	1.085	1.088	1.083	1.086	1.082	θ(F12B11O15)	102.3	102.8	102.2	102.7	102.4	102.8
d(C7H8)	1.091	1.087	1.091	1.085	1.088	1.083	θ(F14B11O15)	106.4	106.8	106.3	106.8	106.3	106.5
d(C7H10)	1.091	1.088	1.090	1.087	1.087	1.085	θ(F13B11O15)	106.0	106.2	105.8	106.0	105.8	106.0
d(B1O5)	1.592	1.579	1.607	1.597	1.597	1.580	θ(B11F12H6)	118.6	121.5	119.0	122.7	118.4	119.4
d(B1F2)	1.351	1.348	1.353	1.352	1.362	1.351	θ(F12H6O5)	165.8	166.9	165.0	165.7	164.4	166.6
d(B1F3)	1.350	1.346	1.353	1.351	1.360	1.349	ϕ(H6O5C7H9)	−174.7	179.7	−173.8	178.9	−175.4	174.5
d(B1F4)	1.421	1.416	1.424	1.420	1.428	1.419	ϕ(H6O5C7H8)	66.9	61.0	67.7	60.2	66.3	55.7
d(O15C17)	1.441	1.439	1.453	1.452	1.458	1.447	ϕ(H6O5C7H10)	−54.2	−59.8	−53.3	−60.5	−54.8	−64.9
d(O15H16)	0.996	0.989	0.997	0.988	0.997	0.988	ϕ(B1O5C7H9)	−49.0	−52.4	−47.7	−51.9	−52.0	−60.0
d(C17H18)	1.090	1.087	1.090	1.085	1.088	1.084	ϕ(B1O5C7H8)	−167.4	−171.1	−166.1	−170.6	−170.4	−178.8
d(C17H19)	1.088	1.085	1.088	1.084	1.086	1.082	ϕ(B1O5C7H10)	71.5	68.1	72.8	68.7	68.6	60.6
d(C17H20)	1.092	1.089	1.092	1.087	1.089	1.086	ϕ(F2B1O5H6)	−55.6	−57.7	−56.0	−58.4	−53.4	−55.6
d(B11O15)	1.590	1.578	1.604	1.595	1.596	1.580	ϕ(F2B1O5C7)	−178.2	174.3	−177.5	172.5	−177.6	178.6
d(B11F12)	1.402	1.398	1.405	1.401	1.409	1.399	ϕ(F3B1O5H6)	179.3	177.4	179.0	176.9	−178.5	179.2
d(B11F13)	1.349	1.345	1.352	1.350	1.359	1.348	ϕ(F3B1O5C7)	53.1	49.3	52.5	47.7	57.3	53.4
d(B11F14)	1.369	1.365	1.373	1.369	1.381	1.370	ϕ(F4B1O5H6)	61.4	59.3	61.2	58.8	63.4	61.2
d(H16F4)	1.591	1.593	1.613	1.627	1.636	1.597	ϕ(F4B1O5C7)	−64.7	−68.8	−65.3	−70.4	−60.7	−64.6
d(H6F12)	1.629	1.630	1.654	1.668	1.673	1.635	ϕ(B1O5H6C7)	−130.2	−132.5	−130.9	−133.9	−128.0	−129.9
d(F2H6)	2.506	2.523	2.523	2.549	2.487	2.500	ϕ(H16O15C17H19)	179.3	174.8	178.8	173.7	−179.4	175.4
d(F4H6)	2.587	2.575	2.601	2.592	2.601	2.578	ϕ(H16O15C17H18)	60.6	56.1	60.0	55.0	62.0	56.6
d(F4H10)	2.769	2.808	2.820	2.872	2.687	2.663	ϕ(H16O15C17H20)	−61.0	−65.2	−61.6	−66.2	−59.5	−64.6
d(F3H9)	2.424	2.454	2.442	2.481	2.467	2.511	ϕ(B11O15C17H19)	−57.2	−57.6	−57.0	−56.8	−58.4	−60.6
d(F12H16)	2.492	2.498	2.502	2.511	2.494	2.499	ϕ(B11O15C17H18)	−175.9	−176.3	−175.8	−175.4	−177.0	−79.4
d(F14H16)	2.583	2.608	2.603	2.642	2.576	2.572	ϕ(B11O15C17H20)	62.4	62.4	62.6	63.3	61.4	59.4
d(F14H20)	2.662	2.718	2.696	2.775	2.622	2.651	ϕ(F12B11O15H16)	−56.2	−54.8	−55.7	−53.4	−56.8	−57.0
d(F13H19)	2.504	2.527	2.533	2.559	2.516	2.531	ϕ(F12B11O15C17)	179.6	177.4	179.5	176.9	−178.5	178.6
θ(C7O5H6)	110.1	110.3	110.0	110.2	109.8	109.8	ϕ(F13B11O15H16)	−176.0	−174.4	−175.5	−173.1	−177.0	−177.1
θ(H9C7O5)	106.0	106.6	105.8	106.5	105.5	106.2	ϕ(F13B11O15C17)	59.8	57.7	59.6	57.2	61.3	58.5
θ(H8C7O5)	107.8	107.7	107.6	107.5	107.2	107.5	ϕ(F14B11O15H16)	60.7	62.2	61.3	63.6	60.0	59.7
θ(H10C7O5)	110.0	110.1	109.8	109.9	109.6	109.8	ϕ(F14B11O15C17)	−63.5	−65.6	−63.6	−66.0	−61.7	−64.6
θ(B1O5C7)	117.4	118.5	117.9	119.3	116.3	117.2	ϕ(B11O15H16C17)	−127.4	−131.2	−128.3	−133.2	−125.1	−127.9
θ(B1O5H6)	109.1	110.0	109.2	110.3	108.3	109.4	ϕ(H16F4B1O5)	−68.7	−63.1	−67.5	−61.6	−73.6	−66.4
θ(F2B1O5)	104.4	104.7	104.3	104.6	104.2	104.6	ϕ(O15H16F4B1)	96.7	76.4	94.2	73.1	103.0	84.8
θ(F3B1O5)	105.8	106.3	105.7	106.1	105.7	106.0	ϕ(C17O15H16F4)	95.5	116.2	97.7	120.1	90.3	107.1
θ(F4B1O5)	104.4	104.9	104.3	104.8	104.4	104.7	ϕ(B11O15H16F4)	−31.9	−14.9	−30.6	−13.1	−34.7	−20.7
θ(C17O15H16)	110.0	110.8	110.1	111.1	109.1	109.7	ϕ(F12H6O5C7)	87.5	80.7	85.0	78.9	89.5	81.1
θ(H18C17O15)	108.0	107.9	107.9	107.7	107.5	107.6	ϕ(F12H6O5B1)	−42.8	−65.7	−45.9	−55.0	−38.4	−48.7
θ(H19C17O15)	106.2	106.8	106.1	106.6	105.8	106.5	ϕ(B11F12H6O5)	−32.4	−19.9	−30.2	−16.9	−36.9	−24.3
θ(H20C17O15)	110.1	110.1	109.9	109.9	109.7	109.8	ϕ(O15B11F12H6)	76.8	70.2	77.1	69.5	79.2	73.4
θ(H16F4B1)	119.4	121.6	120.8	123.3	117.2	119.9	ϕ(O15B11O5B1)	0.8	0.2	0.6	−0.1	1.4	0.8
θ(O15H16F4)	167.0	171.2	167.0	171.0	164.5	169.8	ϕ(F12H6F4H16)	−2.4	−1.3	−1.9	−1.1	−4.2	−2.0

[a] Bond lengths in Å, bond and dihedral angles in degrees; numbering of the atoms as in Figure 5. [b] "Small" and "large" refer to the 6-31G(d) and 6-311++G(3df,2pd) calculations, respectively.

et al.[68] in the solid state. A look to our own MP2 calculations of the different complexes with a small and large basis set shows that the effect of increasing the basis set is to decrease the B−O distance in all cases, which may explain the discrepancy observed by Reetz. Corey et al.[32] were next in giving interesting information regarding the complexes of formyl compounds with boron Lewis acids. They analyzed the X-ray crystallographic data of six complexes of formyl compounds with B−F- or B−O-containing boron Lewis acids and found a definite preference for the conformation in which the formyl group and the B−F or B−O bond are coplanar or nearly so. Their hypothesis was that there is a hydrogen-bond-like interaction between the formyl CH group and the F or O atom in the Lewis acid. More recently, this subject was addressed theoretically by Feng et al.,[70] who performed MP2/6-311++G(2d,p) optimizations and carried out an analysis of the hyperconjugative, relaxation, and steric effects influencing the preference of eclipsed or staggered conformations of formyl compounds interacting with several Lewis acids, BF_3 among them. All these studies provide information on putative hydrogen-bonding interactions where the hydrogen is bound to a carbon atom and the hydrogen bond is the fifth side of a five-membered ring. For btaa, the hydrogen is bound to a much more polarizable oxygen atom, and the hydrogen bond is the sixth side of a six-membered ring, therefore lending extra stability to the complex. In the results obtained by Feng et al.,[70] the difference in the B−F lengths between the hydrogen-bonded F and the other ones is a mere 0.015 Å, and in btaa, the difference is as large as 0.065 Å. This rosy picture is somehow muddled, however, by the different conformations of the six-membered ring predicted by the DFT methods on one side and the MP2 method on the other. Although the eigenvalues of the Hessian are positive in all cases, DFT methods predict a quasi-planar structure for the six-membered ring; in contrast, the MP2 method predicts a more familiar nonplanar (although very slightly so) structure.

As for methanol, acetic acid is dimerized in the gas phase and neat liquid, only much more strongly due to the favorable double-hydrogen-bond interaction. The addition of catalytic amounts of BF_3 should disrupt these dimers, but if the ratio of BF_3 to CH_3COOH concentrations is much lower than 1:1, one should expect some kind of $(CH_3COOH)_2$:BF_3 trimer instead of the btaa monomers. According to Taillandier et al.,[20] this is

TABLE 8: Geometries of the 1:1 btaa Complex

	PBE[b]		B3LYP[b]		MP2[b]	
parameter[a]	small	large	small		small	large
d(C6O7)	1.247	1.241	1.250	1.242	1.253	1.243
d(C6O8)	1.298	1.293	1.307	1.302	1.312	1.301
d(C5C6)	1.487	1.482	1.495	1.489	1.490	1.486
d(O8H12)	1.000	0.991	1.000	0.990	0.998	0.988
d(H10C5)	1.089	1.085	1.089	1.084	1.088	1.083
d(H9C5)	1.094	1.089	1.095	1.089	1.093	1.087
d(H11C5)	1.094	1.092	1.095	1.091	1.092	1.088
d(B1O7)	1.627	1.616	1.652	1.647	1.663	1.640
d(B1F2)	1.415	1.409	1.416	1.409	1.414	1.404
d(B1F3)	1.347	1.345	1.349	1.347	1.352	1.348
d(B1F4)	1.347	1.343	1.349	1.347	1.358	1.342
d(F2H12)	1.568	1.588	1.599	1.637	1.637	1.624
θ(C5C6O7)	120.5	120.4	120.7	120.8	120.8	120.7
θ(C5C6O8)	115.7	116.0	115.5	115.6	114.9	115.3
θ(C6O8H12)	107.1	107.7	107.4	108.4	107.5	107.4
θ(H10C5C6)	110.2	110.2	110.1	110.3	109.8	110.0
θ(H9C5C6)	109.3	110.0	109.4	109.6	108.8	109.4
θ(H11C5C6)	109.3	108.2	109.4	108.8	109.5	108.5
θ(B1O7C6)	127.4	127.9	127.7	128.5	126.3	126.8
θ(F2B1O7)	105.0	105.4	104.7	104.9	104.4	104.9
θ(F3B1O7)	104.2	104.4	103.8	104.0	103.4	103.5
θ(F4B1O7)	104.2	104.5	103.8	104.0	103.3	103.8
θ(F2H12O8)	150.0	149.1	149.4	147.8	147.9	148.6
ϕ(H10C5C6O7)	0.0	−13.7	0.0	−6.6	5.6	−5.3
ϕ(H10C5C6O8)	180.0	167.1	180.0	173.8	−175.0	175.0
ϕ(H9C5C6O7)	−121.4	−136.8	−121.4	−128.8	−114.9	−127.5
ϕ(H11C5C6O7)	121.4	106.0	121.3	114.0	127.5	115.3
ϕ(C5C6O8H12)	180.0	179.4	180.0	179.5	177.7	−177.9
ϕ(C5C6O7B1)	180.0	−177.4	180.0	−179.1	173.7	−174.1
ϕ(O7C6O8H12)	0.0	0.1	0.0	−0.1	−2.9	2.5
ϕ(B1O7C6O8)	0.0	1.8	0.0	0.5	−5.7	5.6
ϕ(F2B1O7C6)	0.0	−4.2	0.0	−1.0	20.0	−18.2
ϕ(F3B1O7C6)	118.3	114.1	118.4	117.5	138.8	99.9
ϕ(F4B1O7C6)	−118.3	−122.7	−118.4	−119.5	−98.1	−137.1
ϕ(B1F2H12O8)	−1.4	−4.1	0.0	−0.9	22.5	−19.5
ϕ(O7B1F2H12)	0.0	3.8	0.0	0.8	−19.9	17.6

[a] Bond lengths in Å, bond and dihedral angles in degrees; numbering of the atoms as in Figure 6. [b] "Small" and "large" refer to the 6-31G(d) and 6-311++G(3df,2pd) calculations, respectively.

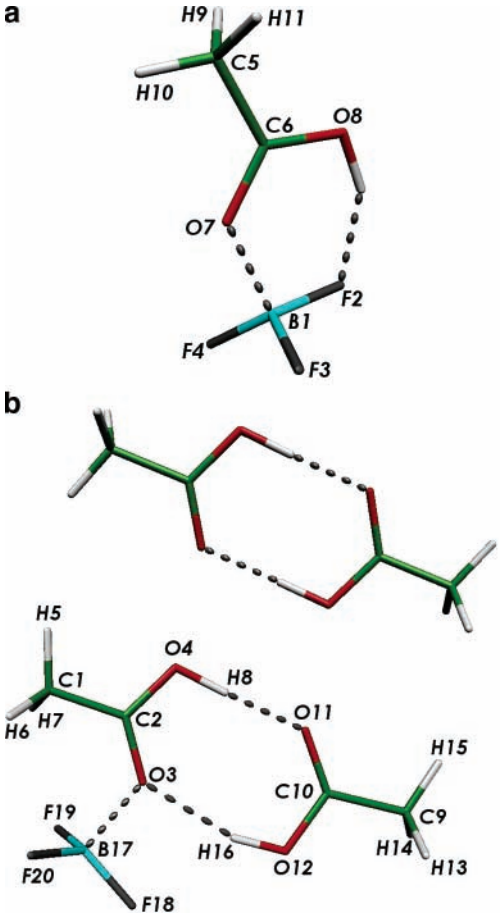

Figure 6. Structure of the 1:1 and 2:1 complexes between CH_3COOH and BF_3: (a) structure and atom numbering for the 1:1 btaa complex; (b) structure and atom numbering of the 2:1 bt2aa complex and comparison to the structure of the acetic acid dimer.

exactly what occurs. They reported the identification of bt2aa using IR spectroscopy and were able to assign the spectrum to a rupture of one of the hydrogen bonds. The structure of the bt2aa trimer with the methods used in this paper is reported in Table 9. The numbering of the atoms in the trimer is also shown in Figure 6. The structure of the acetic acid dimer is shown for comparison, calculated at the same theoretical levels and with the same numbering as bt2aa. Comparing bt2aa with the acetic acid dimer, one sees the following differences: (a) the O···H hydrogen bond opposite to the side of BF_3 bonding contracts about 0.1 Å; (b) the proton-donor OH bond elongates about 0.02 Å; (c) the second O···H bond, next to BF_3, opens considerably, by around 0.3 Å, building up an interaction with one F of the BF_3 moiety, which suffers a very small length increase; and (d) the methyl group of the proton-donor methanol rotates, to maximize the attractive interaction between the F atoms and the H in the methyl group. Comparing bt2aa with btaa, one sees that the BF_3 moiety is less associated (indicated by a larger B···O bond) and does not break the double-hydrogen-bonded structure. The longer hydrogen-bond distance in this complex is comparable to the one in the most favorable conformer of the methanol dimer (about 1.92 Å); in contrast, the other one is shorter than the hydrogen bonds both in the acetic acid dimer and in bt2m.

The NBO point charge analysis for these complexes is shown in Figure 7. The results with the three methods (PBE, B3LYP, and MP2) and the large 6-311++G(3df,2pd) basis set are given, but they show no appreciable difference among them. For the methanol complexes, complexation with BF_3 provokes always a decrease in the formal charge of the oxygen atom to which it is attached. The charge at oxygen, reduced by about 0.06 electrons when btm is formed, is partially restored with the inclusion of the second methanol molecule. Notice that the oxygen in the second methanol molecule of bt2m is more nucleophilic than either the one in btm or the one in free methanol. For acetic acid, the effect of complexation, be it dimer formation or complexation with BF_3, is to equalize approximately the charges on the hydroxyl and carbonyl oxygens.

Infrared Spectra. Most of the information available on the complexes studied comes from either IR or Raman spectroscopies. It is therefore interesting to compare the harmonic frequencies obtained in our calculations with the experimental data available.

Following Taillanier et al.,[20] we explored first the vibrations of the O−BF_3 moiety. The results are presented in Table 10 along with the experimental data. The computational results agree quite well with the experimental measurements, disclosing the pyramidalization of the BF_3 group through the observation of the $\nu_s(BF_3)$ vibration, which is inactive in the IR for isolated BF_3 due to the D_{3h} symmetry of this molecule. The computational results agree also with the important decrease in the frequency of the $\nu_{as}(BF_3)$ antisymmetric vibration, indicating a decrease in the force constant of the BF bonds due to the elongation of the BF bonds (by about 0.04−0.05 Å depending

TABLE 9: Geometries of the bt2aa Trimer and of the Acetic Acid Dimer Calculated at Different Theoretical Levels

	$(CH_3COOH)_2$:BF_3						$(CH_3COOH)_2$					
	PBE[b]		B3LYP[b]		MP2[b]		PBE[b]		B3LYP[b]		MP2[b]	
parameter[a]	small	large	small	large	small	large	small	large	small	large	small	large
d(C1C2)	1.484	1.480	1.492	1.488	1.488	1.484	1.500	1.495	1.507	1.501	1.501	1.497
d(C1H5)	1.089	1.085	1.089	1.084	1.088	1.083	1.094	1.091	1.095	1.090	1.092	1.088
d(C1H6)	1.094	1.091	1.094	1.089	1.092	1.087	1.090	1.086	1.090	1.085	1.089	1.088
d(C1H7)	1.094	1.091	1.094	1.089	1.092	1.087	1.094	1.091	1.095	1.090	1.092	1.083
d(C2O3)	1.256	1.253	1.259	1.254	1.261	1.254	1.227	1.222	1.230	1.223	1.234	1.226
d(C2O4)	1.287	1.279	1.295	1.288	1.301	1.287	1.314	1.307	1.323	1.318	1.332	1.318
d(O3B17)	1.648	1.634	1.678	1.666	1.673	1.653						
d(O4H8)	1.021	1.023	1.019	1.018	1.015	1.015	1.004	1.004	1.004	1.001	1.000	0.997
d(H8O11)	1.566	1.522	1.600	1.565	1.647	1.553	1.655	1.609	1.687	1.657	1.747	1.651
d(C9C10)	1.497	1.491	1.505	1.498	1.499	1.494	1.500	1.495	1.507	1.501	1.501	1.497
d(C9H13)	1.094	1.091	1.095	1.090	1.092	1.088	1.094	1.091	1.095	1.090	1.092	1.088
d(C9H14)	1.094	1.091	1.095	1.090	1.092	1.088	1.094	1.091	1.095	1.090	1.092	1.088
d(C9H15)	1.089	1.085	1.090	1.084	1.088	1.083	1.090	1.086	1.090	1.085	1.089	1.083
d(C10O11)	1.227	1.222	1.230	1.223	1.234	1.226	1.227	1.222	1.230	1.223	1.234	1.226
d(C10O12)	1.316	1.310	1.325	1.320	1.331	1.319	1.314	1.307	1.323	1.318	1.332	1.318
d(O12H16)	0.982	0.977	0.984	0.978	0.985	0.977	1.004	1.004	1.004	1.001	1.000	0.997
d(H16O3)	1.925	1.922	1.951	1.981	1.988	1.917	1.655	1.609	1.687	1.657	1.747	1.651
d(O4O11)	2.586	2.543	2.618	2.581	2.661	2.566	2.659	2.613	2.691	2.658	2.746	2.648
d(O3O12)	2.879	2.882	2.909	2.940	2.944	2.878	2.659	2.613	2.691	2.658	2.746	2.648
d(H16F18)	2.267	2.396	2.305	2.423	2.278	2.378						
d(B17F18)	1.362	1.357	1.363	1.359	1.369	1.358						
d(B17F19)	1.362	1.360	1.364	1.363	1.370	1.361						
d(B17F20)	1.362	1.360	1.364	1.363	1.370	1.361						
θ(C2C1H5)	110.8	110.5	110.8	110.5	110.3	110.1	109.7	109.5	109.7	109.6	109.5	109.3
θ(C2C1H6)	108.4	108.7	108.5	108.9	108.4	108.6	110.0	110.2	110.0	110.1	109.6	110.0
θ(C2C1H7)	108.4	108.7	108.5	108.9	108.4	108.6	109.7	109.5	109.7	109.6	109.5	109.3
θ(H5C1H6)	111.3	111.2	111.2	110.9	111.3	111.2	110.1	110.3	110.1	110.2	110.3	110.4
θ(H5C1H7)	111.3	111.2	111.2	110.9	111.3	111.2	107.2	107.1	107.2	107.2	107.6	107.5
θ(H6C1H7)	106.3	106.4	106.5	106.6	107.0	107.0	110.1	110.3	110.1	110.2	110.3	110.4
θ(C1C2O3)	123.1	123.2	123.2	123.5	123.7	123.4	122.6	122.6	122.8	122.9	123.3	123.1
θ(C1C2O4)	117.4	117.3	117.2	116.9	116.9	116.9	113.1	113.6	113.0	113.4	112.4	113.0
θ(O3C2O4)	119.4	119.4	119.6	119.6	119.4	119.6	124.3	123.9	124.3	123.7	124.3	123.9
θ(C2O3B17)	125.5	125.9	126.0	126.8	124.8	125.1						
θ(C2O4H8)	109.9	111.5	110.1	111.9	109.0	110.2	109.9	110.5	110.0	110.8	109.1	109.4
θ(C10C9H13)	109.6	109.4	109.6	109.5	109.4	109.2	109.7	109.5	109.7	109.6	109.5	109.3
θ(C10C9H14)	109.6	109.4	109.6	109.5	109.4	109.2	109.7	109.5	109.7	109.6	109.5	109.3
θ(C10C9H15)	110.0	110.2	109.9	110.1	109.6	110.0	110.0	110.2	110.0	110.1	109.6	110.0
θ(H13C9H14)	107.2	107.1	107.2	107.2	107.6	107.5	107.2	107.1	107.2	107.2	107.6	107.5
θ(H13C9H15)	110.2	110.4	110.2	110.3	110.4	110.5	110.1	110.3	110.1	110.2	110.3	110.4
θ(H14C9H15)	110.2	110.4	110.2	110.3	110.4	110.5	110.1	110.3	110.1	110.2	110.3	110.4
θ(C9C10O11)	122.4	122.7	122.6	123.0	123.0	123.1	122.6	122.6	122.8	122.9	123.3	123.1
θ(C9C10O12)	112.5	113.1	112.4	113.0	111.9	112.6	113.1	113.6	113.0	113.4	112.4	113.0
θ(O11C10O12)	125.1	124.1	124.9	124.0	125.1	124.3	124.3	123.9	124.3	123.7	124.3	123.9
θ(H8O11C10)	133.4	131.5	133.2	132.1	134.9	132.3	124.7	124.6	124.9	125.2	125.9	125.4
θ(C10O12H16)	111.6	111.4	111.6	111.7	110.9	110.4	109.9	110.5	110.0	110.8	109.1	109.4
θ(O12H16F18)	130.6	129.6	130.3	130.8	131.6	128.7						
θ(O3B17F18)	99.6	100.6	99.3	100.3	99.0	99.9						
θ(O3B17F19)	104.8	105.3	104.3	104.9	104.4	104.8						
θ(O3B17F20)	104.8	105.3	104.3	104.9	104.4	104.8						
θ(F18B17F19)	115.3	114.8	115.6	115.1	115.6	115.3						
θ(F18B17F20)	115.3	114.8	115.6	115.1	115.6	115.3						
θ(F19B17F20)	114.5	114.1	114.8	114.3	114.9	114.4						
θ(H16F18B17)	94.6	92.3	95.2	93.9	96.6	93.0						
ϕ(H5C1C2O3)	180.0	180.0	180.0	180.0	180.0	180.0	−121.3	−121.4	−121.2	−121.3	−121.1	−121.3
ϕ(H5C1C2O4)	0.0	0.0	0.0	0.0	0.0	0.0	58.7	58.6	58.8	58.7	58.9	58.7
ϕ(H6C1C2O3)	−57.5	−57.7	−57.6	−57.9	−57.9	−58.0	0.0	0.0	0.0	0.0	0.0	0.0
ϕ(H6C1C2O4)	122.5	122.3	122.4	122.1	122.0	122.0	180.0	180.0	180.0	180.0	180.0	180.0
ϕ(H7C1C2O3)	57.5	57.7	57.6	57.9	57.9	58.0	121.3	121.4	121.2	121.3	121.1	121.3
ϕ(H7C1C2O4)	−122.5	−122.3	−122.4	−122.1	−122.0	−122.0	−58.7	−58.6	−58.8	−58.7	−58.9	−58.7
ϕ(C1C2O3B17)	0.0	0.0	0.0	0.0	0.0	0.0						
ϕ(O4C2O3B17)	180.0	180.0	180.0	180.0	180.0	180.0						
ϕ(C1C2O4H8)	180.0	180.0	180.0	180.0	180.0	180.0	180.0	180.0	180.0	180.0	180.0	180.0
ϕ(O3C2O4H8)	0.0	0.0	0.0	0.0	0.0	0.0	0.0	0.0	0.0	0.0	0.0	0.0
ϕ(C2O3B17F18)	180.0	180.0	180.0	180.0	180.0	180.0						
ϕ(C2O3B17F19)	60.5	60.4	60.4	60.4	60.5	60.4						
ϕ(C2O3B17F20)	−60.5	−60.4	−60.4	−60.4	−60.5	−60.4						
ϕ(C2O4O11C10)	0.0	0.0	0.0	0.0	0,0	0.0	0.0	0.0	0.0	0.0	0.0	0.0
ϕ(H13C9C10O11)	121.3	121.5	121.3	121.4	121.2	121.4	121.3	121.4	121.1	121.3	121.1	121.3
ϕ(H13C9C10O12)	−58.7	−58.5	−58.7	−58.6	−58.8	−58.6	−58.7	−58.6	−58.8	−58.7	−58.9	−58.7
ϕ(H14C9C10O11)	−121.4	−121.5	−121.2	−121.4	−121.2	−121.4	−121.3	−121.4	−121.2	−121.3	−121.1	−121.3
ϕ(H14C9C10O12)	58.6	58.5	58.8	58.6	58.8	58.6	58.7	58.6	58.8	58.7	58.9	58.7

TABLE 9: (Continued)

	$(CH_3COOH)_2$:BF_3						$(CH_3COOH)_2$					
	PBE[b]		B3LYP[b]		MP2[b]		PBE[b]		B3LYP[b]		MP2[b]	
parameter[a]	small	large	small	large	small	large	small	large	small	large	small	large
ϕ(H15C9C10O11)	0.0	0.0	0.0	0.0	0.0	0.0	0.0	0.0	0.0	0.0	0.0	0.0
ϕ(H15C9C10O12)	180.0	180.0	180.0	180.0	180.0	180.0	180.0	180.0	180.0	180.0	180.0	180.0
ϕ(C9C10O11H8)	180.0	180.0	180.0	180.0	180.0	180.0	180.0	180.0	180.0	180.0	180.0	180.0
ϕ(O12C10O11H8)	0.0	0.0	0.0	0.0	0.0	0.0	0.0	0.0	0.0	0.0	0.0	0.0
ϕ(C9C1O12H16)	180.0	180.0	180.0	180.0	180.0	180.0	180.0	180.0	180.0	180.0	180.0	180.0
ϕ(O11C10O12H16)	0.0	0.0	0.0	0.0	0.0	0.0	0.0	0.0	0.0	0.0	0.0	0.0
ϕ(C10O12H16F18)	180.0	180.0	180.0	180.0	180.0	180.0						
ϕ(O12H16F18B17)	180.0	180.0	180.0	180.0	180.0	180.0						
ϕ(O3B17F18H16)	0.0	0.0	0.0	0.0	0.0	0.0						
ϕ(F19B17F18H16)	111.5	112.5	110.9	112.6	110.8	111.6						
ϕ(F20B17F18H16)	−111.5	−112.5	−110.9	−112.6	−110.8	−111.6						

[a] Bond lengths in Å, bond and dihedral angles in degrees; numbering of the atoms as in Figure 6. [b] "Small" and "large" refer to the 6-31G(d) and 6-311++G(3df,2pd) calculations, respectively.

on the complex) and the breaking of the symmetry due to the inequivalence of the different BF bonds.

The second important piece of information that can be derived from both the experimental and the theoretical studies concerns the hydrogen-bonding interactions. Taillandier et al.[20] measured the spectra of solutions of BF_3 in methanol, starting from pure CH_3OH and going all the way to the 1:1 concentration ratio. The results show that the vibration ν(OH) appearing at 3325 cm^{-1} in pure liquid CH_3OH broke down into two signals, one between 3570 and 3545 cm^{-1} and another between 3287 and 3200 cm^{-1}, depending on the ratio of concentrations. The high-frequency band increases its intensity up to the point when the ratio $[CH_3OH]/[BF_3]$ is 2:1 and then decreases again until it is completely absent when the ratio is 1:1. Thus, the authors conclude that this band belongs to the 2:1 complex. Our results are compared to the experimental ones in Table 11.

A first comparison between the theoretical and experimental data can be done with respect to the methanol monomer and dimer. Besides the obvious observation that the frequencies are a couple of hundred cm^{-1} off, a consequence of anharmonicity, one sees that there is also a discrepancy with respect to the frequency shifts. These are less affected by anharmonicity and should reflect better the experimental situation. A blue-shifted frequency for the OH frequency of the proton-acceptor monomer was measured by both Coussan et al., in an Ar matrix,[48] and Huisken et al., in the gas phase,[63] but the calculations produce a red shift of approximately the same magnitude. All experimental and theoretical experiments predict a red shift of ν(OH) for the proton donor, but the experimental shift is smaller than the one predicted theoretically. The two discrepancies between experimental and theoretical data stem mainly from the lack of anharmonicity effects in the calculations, which are strong for the OH bonds. We included in Table 11 some partial results obtained including anharmonicity in the frequencies through the numerical calculation of third derivatives. The frequencies and the frequency shifts in the dimer are now much more in agreement with the experimental results, including the observed blue shift. A full report of these results is given elsewhere.[71]

Methanol associates strongly in the liquid, and consequently, the ν(OH) frequency measured in neat CH_3OH is much more red-shifted[20] than that obtained for the dimer in the gas phase. We have not calculated the spectra of open-chain trimers or tetramers, but we expect this same trend to be observed in the calculations on the basis of the evidence we discuss below for the $(btm)_2$ tetramer and the bt2m trimer.

The ν(OH) band in the 1:1 btm dimer has been measured by Taillandier et al.[20] and by Deroualt et al.,[19] adding BF_3 to pure methanol. In these conditions, one can expect that the dimer is further associated, as we have discussed before. Thus, the observed experimental frequency should not correspond to the frequency calculated for the isolated complex. This is exactly the case, as can be seen in Table 11. BF_3 complexation induces a small red shift in the frequency, about 5 or more times smaller than the experimental one. Observe that the experimental red shift is comparable to that observed for liquid methanol, suggesting strongly the association by a similar mechanism, as proposed in the experimental references.[19,20] In fact, if we look at the $(btm)_2$ dimer, we see a much more strongly red-shifted signal. Even after one accepts that the calculated results exaggerate the red shift, these results are not in agreement with the experimental ones. Only one signal is observed experimentally, and two (asymmetric and symmetric vibrations) are predicted computationally if the closed tetramer would be the one present in solution. This is another argument against the presence of the closed tetramer in solutions at the 1:1 concentration ratio and in favor of the open chains proposed by experimentalists.[19,20]

The situation is more complicated with regard to the bt2m trimer. Although the experimental red shift of the ν(OH) band of the proton-donor methanol monomer is comparable to that found in the methanol dimer in the gas phase, and reasonably in agreement with the calculations, this is not so for the ν(OH) band of the proton-acceptor methanol monomer. Experimentally, this band is considerably more red-shifted than the one in liquid methanol or the one in the 1:1 dimer associated through hydrogen bonding. The same, only much more so, can be said of the calculations. The experimental work did not find evidence of further association of the trimers. Thus, we believe that the discrepancy between the experimental and theoretical data may be due to exaggeration of the red shift in the calculations concurrently with the effect of the other molecules surrounding the trimer in the experimental case. Nonetheless, the data support the structure discussed for the trimer with a strong F···H interaction. We think that, were the ν(OH) frequency shift to be investigated in the gas phase or a nonassociative solvent, the red shift would be larger than that observed before,[19,20] although probably not so large as predicted in our calculations.

Thermochemical Properties. An important consideration for the final goals of our study is the relative stability of the different complexes. The results with the different methods are shown in Table 12. Counterpoise corrections were obtained for the internal energy and used in the calculation of thermodynamic properties. No correction was used for geometries or frequencies.

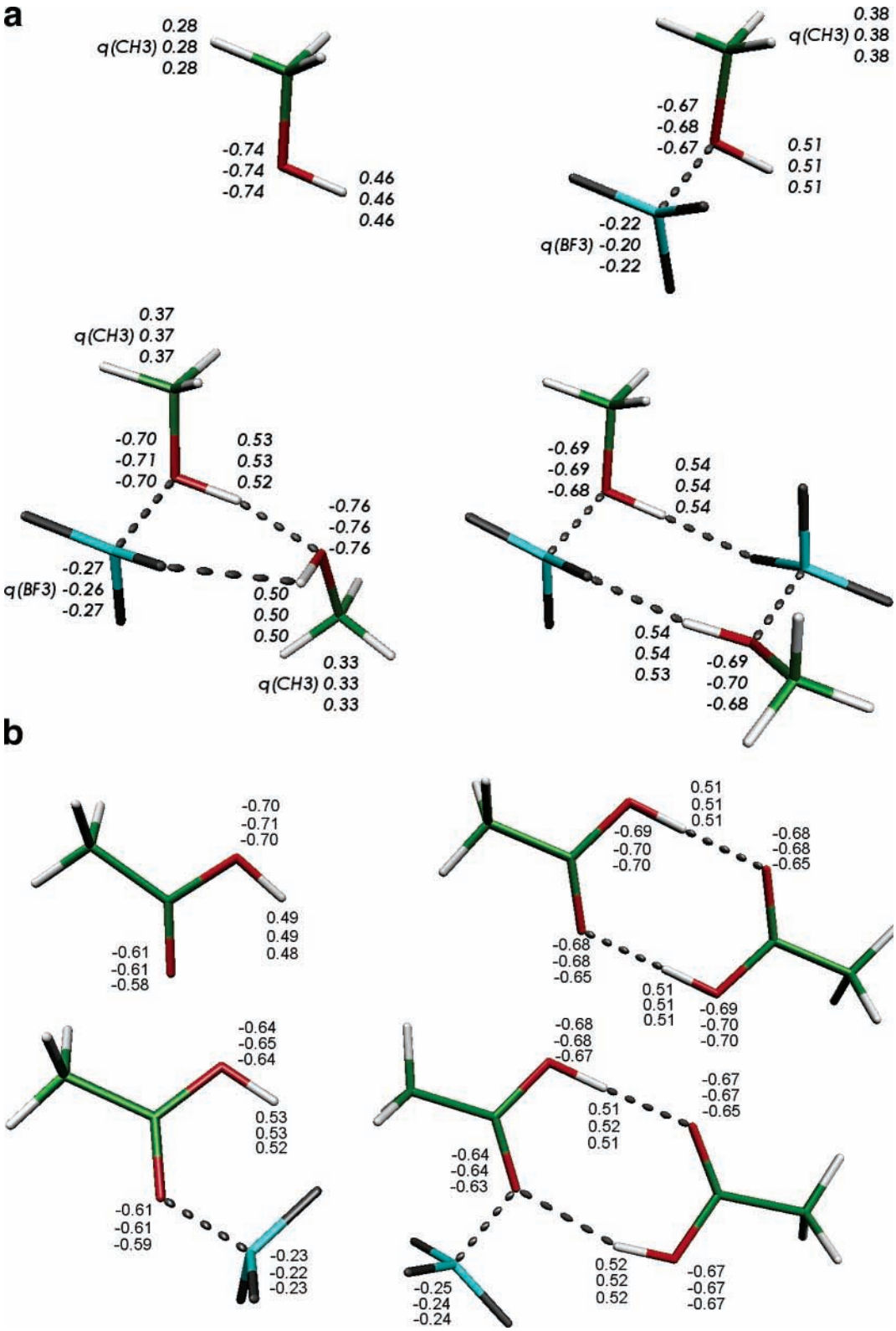

Figure 7. Point charges derived from the NBO analysis for the different species studied.

The absolute values of energies, enthalpies, and free energies can be obtained from the authors.

The first experimental data available seem to be the enthalpies of formation of the etherates btdme and btdee. The $(CH_3)_2O$:BF_3 complex was found to be slightly more stable than the $(CH_3CH_2)_2O$:BF_3 etherate in all these older studies. This conclusion was also supported in a paper of Rutenberg et al.[72] where they reported a NMR study of the exchange of BF_3 between both etherates, concluding that BF_3 shows a preference for dimethyl ether. The fact that DME behaves as a stronger Lewis base than DEE toward the Lewis acid BF_3 is a bit anomalous and has been ascribed to steric interactions. In fact, VanDyke and MacDiarmid[73] studied the relative basicity of both ethers toward other less bulky Lewis acids and concluded that they exhibit the expected basicity (i.e., DME less basis than DEE). Moreover, Gore and Danyluk[74] performed a study of the NMR chemical

TABLE 10: Comparison of Experimental and Calculated IR Frequencies Affecting the BF_3 Moiety in the Different Complexes[a]

species	method	$\nu_s(BF_3)$	$\nu_{as}(BF_3)$	$\nu(O-B)$[e]
BF_3 free	exptl[b]	888	1454 (^{11}B)	
	PBE	897	1469	
	B3LYP	886	1445	
	MP2	891	1464	
btm	exptl[b]	853 (−35)	1220−1162 (−234, −292)	693
	exptl solid[c]	890	1220−1130	717
	exptl liquid[c]	860 (−28)	1224−1165 (−230, −289)	696
	PBE	850 (−47)	1296−1261 (−173, −208)	620
	B3LYP	833 (−53)	1283−1248 (−162, −197)	604
	MP2	843 (−48)	1298−1256 (−166, −208)	628
bt2m	exptl[b]	867 (−21)	1210−1145 (−244, −309)	689
	PBE	859 (−38)	1295−1225 (−174, −244)	679
	B3LYP	836 (−50)	1272−1205 (−173, −240)	657
	MP2	856 (−35)	1302−1229 (−162, −235)	685
btaa	exptl[b]	852 (−36)	∼1162 (−292)	632, 728
	PBE	822 (−75)	1141 (−328)	655, 691
	B3LYP	805 (−81)	1130 (−315)	631, 672
	MP2	817 (−74)	1154 (−310)	645, 682
bt2aa	exptl[b]			
	PBE	849 (−48)	1232 (−237)	631
	B3LYP	830 (−56)	1218 (−227)	616
	MP2	838 (−53)	1241 (−223)	627
btdme	exptl (N_2)[d]	817.1 (−71)	1240−1208 (−214, −246)	652.5
	exptl (Ar)[d]	815.1 (−73)	1252−1223 (−202, −231)	637.8
	exptl (liq)[f]	805 (−83)	1177−1216 (−277, −238)	661
	PBE	832 (−65)	1288−1250 (−181, −219)	624
	B3LYP	810 (−76)	1274−1234 (−171, −211)	604
	MP2	827 (−64)	1289−1240 (−175, −224)	636
btdee	exptl (liq)[f]	831 (−57), 879 (−9)	1252−1210 (−202, −244)	664
	PBE	821 (−76), 890 (−7)	1273−1234 (−196, −235)	635
	B3LYP	817 (−69), 876(−10)	1253−1227 (−192, −218)	612
	MP2	827 (−64), 889 (−2)	1272−1223 (−192, −241)	647
bteox	PBE	830 (−67)	1316−1258 (−153, −211)	611
	B3LYP	807 (−79)	1300−1245 (−145, −200)	591
	MP2	821 (−70)	1314−1254 (−150, −210)	618

[a] Only the theoretical values obtained with the 6-311++G(3df,2pd) basis set are presented. [b] Reference 20. [c] Reference 19. [d] In cryogenic matrixes, ref 34. [e] Actually coupled to $\nu_s(BF_3)$ and torsions of the CH_n groups. [f] Reference 75.

TABLE 11: Comparison of Experimental and Theoretical Results for the ν(OH) Band of the $CH_3OH:BF_3$ Species

description		experimental	PBE/large	B3LYP/large	MP2/large
MeOH monomer		3679[a]	3917 (37/53/62)[d]	3856 (32/55/63)[d]	3910 (42/41/54)[d]
		3642[b]	3738[n]		
		3667[c]			
associated liquid		3324[e] (−355)[f]			
MeOH dimer	acceptor	3655[j] (−12)[m]	3907 (−10)[f]	3848 (−8)[f]	3900 (−10)[f]
		3679[k] (+12)[m]	3719 (−19)[n]		
		3684[l] (+5)[f]			
	donor	3519[j] (−148)[m]	3726 (−191)[f]	3693 (−163)[f]	3746 (−164)[f]
		3527[k] (−140)[m]	3559 (−179)[n]		
		3574[l] (−105)[f]			
1:1 complex btm		3303[e] (−376)[f]	3857[h] (−60)[f]	3808[h] (−48)[f]	3839[h] (−71)[f]
		3335[g] (−344)[f]	3425[i] (−492)[f]	3435[i] (−421)[f]	3465[i] (−465)[f]
			3336[i] (−581)[f]	3353[i] (−503)[f]	3378[i] (−523)[f]
2:1 complex bt2m	acceptor	3570−3545[e] (∼−120)[f]	3811 (−106)[f]	3774 (−82)[f]	
		3545[g] (−120)[f]			
	donor	3287−3200[e] (∼−440)[f]	3005 (−912)[f]	3086 (−770)[f]	
		3245[g] (−434)			

[a] The gas phase, ref 20. [b] In CCl_4, ref 20. [c] Ar matrix, ref 62. [d] Values in parentheses give the relative intensities of the ν(OH) and $\nu(CH_3)$ bands. [e] Reference 20. [f] Shift with respect to the monomer in the gas phase. [g] Reference 19. [h] From the 1:1 dimer. [i] From the $(CH_3OH:BF_3)_2$ tetramer and antisymmetric and symmetric vibrations respectively. [j] N_2 matrix, ref 55; the A isomer has been chosen because it is the one present at lower temperatures and thus would be more comparable to the theoretical calculations. [k] Ar matrix, ref 48. [l] The gas phase, ref 63. [m] Shift with respect to the monomer in an Ar matrix. [n] Anharmonic values calculated at the PBE/6-311++G(3df,2pd) level, ref 71.

shifts of three BF_3 etherates in dichloromethane at 23 °C and found, in marked disagreement with the previous work, that btdme is less stable than btdee. From these results, they concluded that the relative stability is probably influenced by the different solvents used in the experiments. Maria and Gal[12] studied calorimetrically the complexes of BF_3 with a lot of nonprotogenic solvents, including DEE but not DME, in CH_2Cl_2 and nitrobenzene. The enthalpies of complexation obtained for btdee are considerably higher because they include the effects of the solvent phase change, of the BF_3 complexation with the solvent, and of complex solvation. Not all these effects can be independently evaluated; thus, we cannot compare the experimental results of Maria and Gal[12] with the ones obtained theoretically here. On the other side, Fărcaşiu et al.[18] derived

TABLE 12: Relative Energies, Standard Enthalpies, and Free Energies at 298.15 K (in kJ/mol) for the Complexes Studied

		PBE		B3LYP		MP2	
species	property[a]	6-31G(d)	6-311++G(3df,2pd)	6-31G(d)	6-311++G(3df,2pd)	6-31G(d)	6-311++G(3df,2pd)
$(Met)_2$	$\Delta(E+ZPE)$	−25.9	−17.0	−24.4	−15.1	−26.8	−20.3
	$H(298)$	−25.6	−16.0	−24.0	−14.0	−26.3	−19.1
	$G(298)$	4.1	9.5	5.4	11.5	3.1	5.2
	$\Delta(E+ZPE)$ cp	−15.6	−17.2	−24.4	−15.2	−26.6	−16.9
	$\Delta H(298)$ cp	−15.3	−14.7	−12.5	−12.8	−12.0	−15.7
	$\Delta G(298)$ cp	13.5	10.8	16.3	12.5	16.7	9.0
btm	$\Delta(E+ZPE)$	−58.0	−44.1	−47.7	−32.0	−63.5	−59.5
	H(298)	−60.1	−43.9	−49.5	−33.8	−65.8	−53.2
	G(298)	−19.7	−5.6	−10.3	6.0	−24.9	−11.5
	$\Delta(E+ZPE)$ cp	−33.2	−39.0	−20.7	−27.4	−23.9	−45.9
	$\Delta H(298)$ cp	−35.3	−38.9	−22.5	−29.2	−26.1	−39.6
	$\Delta G(298)$ cp	5.2	−0.5	16.7	10.5	14.8	2.2
bt2m	$\Delta(E+ZPE)$	−105.5	−80.3	−92.6	−63.6	−112.0	−99.8
	$H(298)$	−109.4	−82.0	−96.5	−67.2	−115.9	−95.5
	$G(298)$	−54.7	−28.6	−41.9	−13.4	−61.3	−37.4
	$\Delta(E+ZPE)$ cp	−68.3	−71.5	−40.1	−56.8	−40.7	−79.7
	$\Delta H(298)$ cp	−72.2	−74.7	−55.3	−61.7	−58.7	−75.4
	$\Delta G(298)$ cp	−16.5	−21.3	−0.2	−7.8	−3.3	−17.7
$(btm)_2$	$\Delta(E+ZPE)$	−97.8	−75.2	−93.8	−67.7	−99.4	−85.4
	$H(298)$	−98.5	−75.6	−95.0	−68.4	−99.7	−85.7
	$G(298)$	−49.6	−28.5	−44.0	−20.7	−52.3	−38.9
	$\Delta(E+ZPE)$ cp	−72.4	−79.2	−64.3	−65.9	−62.4	−68.5
	$\Delta H(298)$ cp	−73.1	−79.7	−65.5	−66.7	−62.7	−68.9
	$\Delta G(298)$ cp	−24.1	−32.5	−14.5	−18.9	−15.3	−22.1
$(AcA)_2$	$\Delta(E+ZPE)$	−80.9	−68.1	−76.8	−60.3	−71.7	−65.2
	$H(298)$	−81.1	−68.2	−76.9	−60.4	−71.4	−65.2
	$G(298)$	−39.0	−26.7	−34.9	−19.1	−30.3	−24.0
	$\Delta(E+ZPE)$ cp	−65.2	−65.7	−59.1	−58.3	−49.5	−56.5
	$\Delta H(298)$ cp	−65.2	−65.8	−59.0	−58.4	−49.2	−56.5
	$\Delta G(298)$ cp	−24.5	−24.5	−18.6	−17.2	−8.7	−15.3
btaa	$\Delta(E+ZPE)$	−51.6	−57.5	−38.9	−41.0	−62.9	−62.6
	$H(298)$	−75.1	−56.6	−62.5	−42.2	−64.2	−55.3
	$G(298)$	−40.1	−20.6	−23.1	−3.4	−23.6	−15.0
	$\Delta(E+ZPE)$ cp	−23.6	−52.1	−7.2	−36.2	−20.0	−46.3
	$\Delta H(298)$ cp	−47.1	−51.2	−30.8	−37.4	−21.3	−39.0
	$\Delta G(298)$ cp	−12.1	−15.2	8.6	1.4	19.3	1.3
bt2aa	$\Delta(E+ZPE)$	−135.2	−111.0	−119.4	−88.8	−124.9	−122.0
	$H(298)$	−135.7	−109.3	−119.6	−89.0	−125.0	−113.9
	$G(298)$	−50.3	−26.4	−35.0	−4.9	−41.4	−28.3
	$\Delta(E+ZPE)$ cp	−90.7	−102.4	−69.8	−81.1	−59.4	−96.9
	$\Delta H(298)$ cp	−91.1	−100.7	−70.0	−81.4	−59.4	−88.8
	$\Delta G(298)$ cp	−2.1	−17.8	14.6	2.7	24.1	−3.2
btdme	$\Delta(E+ZPE)$	−58.6	−47.5	−48.0	−46.5	−70.8	−71.7
	$H(298)$	−60.0	−46.7	−49.1	−36.3	−72.4	−64.9
	$G(298)$	−17.3	−6.1	−7.2	5.9	−29.2	−20.5
	$\Delta(E+ZPE)$ cp	−31.8	−41.4	−18.9	−44.0	−26.3	−54.8
	$\Delta H(298)$ cp	−33.2	−40.6	−20.0	−33.8	−27.8	−47.9
	$\Delta G(298)$ cp	9.5	0.1	21.9	8.4	15.4	−3.6
btdee	$\Delta(E+ZPE)$	−65.7	−54.2	−54.8	−41.0	−78.9	−80.3
	$H(298)$	−66.5	−52.8	−55.5	−41.7	−80.1	−72.9
	$G(298)$	−24.0	−11.9	−13.1	0.9	−35.9	−27.4
	$\Delta(E+ZPE)$ cp	−30.9	−43.5	−18.6	−34.8	−23.7	−56.4
	$\Delta H(298)$ cp	−31.7	−42.1	−19.3	−35.5	−24.8	−49.0
	$\Delta G(298)$ cp	7.1	−5.0	19.5	3.3	15.7	−7.2
bteox	$\Delta(E+ZPE)$	−52.7	−42.1	−43.7	−31.2	−61.9	−70.0
	$H(298)$	−54.2	−41.3	−44.9	−32.3	−63.6	−54.8
	$G(298)$	−12.3	−1.6	−3.8	8.8	−21.0	−11.8
	$\Delta(E+ZPE)$ cp	−29.2	−38.5	−18.0	−26.1	−21.7	−54.9
	$\Delta H(298)$ cp	−30.7	−37.7	−19.2	−27.3	−23.5	−39.8
	$\Delta G(298)$ cp	11.2	2.0	21.9	13.8	19.1	3.3

[a] The symbol "cp" after a property indicates that it has been corrected for basis set superposition error by including the counterpoise correction.

an enthalpy of activation of −40.5 kJ/mol and maintain that this is a good estimation of the strength of the BF_3−DEE interaction (our average value is −42.2 kJ/mol). From the theoretical point of view, Jonas et al.[13] calculated D_0 for the btdme complex at the MP2/TZ2P level, obtaining a value of −62.3 kJ/mol at 0 K. This value is not counterpoise corrected, and as we can see in Table 11, this correction is important for the MP2 calculations. Rauk et al.[14] at the MP2/6-31G(d) level obtained a similarly large value, −72.0 kJ/mol at 0 K. Our average value for D_0 using the 6-311++G(3df,2pd) basis set is −44.9 kJ/mol when corrected for BSSE (the uncorrected average value is −55.8 kJ/mol).

The information about the other complexes we studied is even scarcer. The only available information concerns the methanol and the acetic acid dimers. In the first case, the papers by Fileti and Canuto[54] and by Tsuzuki et al.[50] suggest a CCSD(T) limit

D_o of about −17.1 kJ/mol, completely in agreement with our three counterpoise-corrected large-basis-set results obtained with the PBE, B3LYP, and MP2 methods (average value −16.4 kJ/mol). For the acetic acid dimer, the paper by Chocholoušová et al.[64] summarizes previously existing information about the stability of the dimer, quoting the dimerization energy as −62.7 kJ/mol and the free energy of dimerization as −17 kJ/mol. Both results agree with those we show in Table 11 (average zero-point energy (ZPE)-corrected dimerization energy −60.2 kJ/mol and average free energy of dimerization −19.0 kJ/mol). In view of the scarcity of other data and the agreement between our calculated results and those available either theoretically or experimentally for the methanol and acetic acid dimers, it looks reasonable to process the discussion as if the calculated data do actually reflect the relative stability of the other complexes.

Looking first to the etherates, one sees that all theoretical methods predict uniformly that btdee is more stable than btdme. The difference is quite small, however, about 4−5 kJ/mol in favor of the former. The enormous importance of the entropic contribution to the free energy makes both etherates in the gas phase at room temperature able to dissociate with relative ease, although the energy of dimerization is pretty high. Due to the relatively similar free energies of complexation, a mixture of any of the etherates with oxirane should tend to establish an equilibrium with the presence of both BF_3 complexes (an equilibrium that would be broken if oxirane starts to polymerize, of course).

However, the situation is more complicated when one mixes the etherates with acetic acid or methanol. Looking to the equilibrium

$$\mathrm{DEE{:}BF_3} + \mathrm{Met} \rightarrow \mathrm{DEE} + \mathrm{btm} \qquad (1)$$

one gets a $\Delta_r G^\circ_{298}(1)$ of 4.4, 7.2, and 9.4 kJ/mol using the three methods with the 6-311++G(3df,2pd) basis set, concluding that the equilibrium is displaced to the side of the etherate, not to the side of btm if all the species are in a similar concentration.

For acetic acid,

$$\mathrm{DEE{:}BF_3} + \mathrm{AcA} \rightarrow \mathrm{DEE} + \mathrm{btaa} \qquad (2)$$

one gets a $\Delta_r G^\circ_{298}(2)$ of −10.2, −1.9, and 8.5 kJ/mol, showing a larger variation with the method than for methanol but suggesting anyway that the equilibrium is now more displaced toward the formation of btaa.

The situation, then, is not the same for methanol as compared to acetic acid. In the first case, the 1:1 btm complex is less stable (in terms of free energy) than the btdee etherate, which would tend to dominate the relation. However, the trimer bt2m is much more stable than btdee and would tend to form even when methanol is not in excess in the mixture. In fact, if one looks to the equilibrium

$$\mathrm{DEE{:}BF_3} + (\mathrm{Met})_2 \rightarrow \mathrm{DEE} + \mathrm{bt2m} \qquad (3)$$

one gets a $\Delta_r G^\circ_{298}(3)$ of −16.3, −11.1, and −10.4 kJ/mol, in favor of the transfer of the boron trifluoride species to the methanol dimer.

For the acetic acid complex, btaa has a lower counterpoise corrected free energy than btdee (except at the MP2 level) so that CH_3COOH would have not too many problems for sequestering the BF_3 from the etherate. The main problem is that the free energy of btaa is much higher than that of the acetic acid dimer so that no acetic acid monomer would be available to confiscate BF_3 from the etherate. However, the enthalpy of complexation of the bt2aa trimer is so high that it overrules the unfavorable entropy contribution, and the free energy of the trimer is larger than both the free energy of the acetic acid dimer and of the etherate. We can write then

$$\mathrm{DEE{:}BF_3} + (\mathrm{AcA})_2 \rightarrow \mathrm{DEE} + \mathrm{bt2aa} \qquad (4)$$

for which $\Delta_r G^\circ_{298}(4)$ is positive, 11.6, 16.6, and 19.4 kJ/mol. This means that the equilibrium would not favor the formation of bt2aa in the same way that it was favoring the formation of bt2m. Thus, the conclusion of this thermochemical analysis is that the mixture of either methanol or acetic acid with BF_3 etherate into an inert solvent would lead to the appearance of bt2m and btaa, respectively.

There is another possible way to look to this problem, which consists of investigating the equilibrium

$$\mathrm{X_2} + 2\mathrm{X{:}BF_3} \rightarrow 2\mathrm{X_2{:}BF_3} \qquad (5)$$

where X is either AcA or Met. In the first case, the enthalpies of reaction at 298.15 K calculated using the 6-311++G(3df,2pd) basis set and the three theoretical methods are −33.2, −29.2, and −43.1 kJ/mol, and in the second case, they are −56.9, −52.2, and −56.9 kJ/mol, all in favor of the trimers. However, the calculation of the free energy of reaction shows a different picture. In contrast, for methanol, it favors clearly the displacement of the equilibrium to the side of the trimers (−52.4, −71.5, and −57.5 kJ/mol); for acetic acid, the equilibrium is displaced to the side of the dimers (19.2, 19.8, and 6.4 kJ/mol), leading to the same conclusion (that the species to be found should be bt2m and btaa).

Effects of Basis Set and Level of Calculation. The calculations performed with different theoretical methods do afford different values for the properties studied. Differences between the two basis sets employed are quite clear especially in the calculation of the thermochemical values. Counterpoise (cp) corrections performed on the calculations using the smallest basis set do improve the results but not nearly enough. The difference with the results obtained using the largest basis set within each methodology is quite large. Basis set superposition errors are also present in the calculations done with the largest basis set, although at a much more tolerable level. MP2 calculations exhibit the largest difference between the uncorrected and cp-corrected value, several times larger than the effect noticeable in the DFT calculations, a known effect of the faster convergence of DFT results with the extension of the basis set. There is no clear-cut tendency in the results with respect to the methods. Sometimes PBE and MP2 give similar results, and sometimes, B3LYP affords results nearer to MP2. Differences are not dramatic (on the order of 10 kJ/mol at most) but are sufficiently important to matter given the small free energies of these complexes in the gas phase.

Ring Opening of Epoxides. What can we say with respect to ring opening of epoxides in light of the previous discussion? It is clear that neither of these small molecules is representative of the ones the organic chemists are usually interested in. Nonetheless, it is suggestive that for species with more or less the same degree of complexity (methanol, acetic acid, methyl and ethyl ethers, oxirane) the emerging view is that the Lewis acid would be transferred from the original etherate complex to the nucleophile instead of to the epoxide as conventional wisdom would have it. In fact, using the previous results, we can look at the equilibria for methanol as

$$DEE{:}BF_3 + EOX + (Met)_2 \rightarrow DEE + bteox + (Met)_2 \quad (6a)$$

$$DEE{:}BF_3 + EOX + (Met)_2 \rightarrow DEE + EOX + bt2m \quad (6b)$$

obtaining a $\Delta_rG°_{298}$(6a) of 7.0, 10.5, and 10.5 kJ/mol; $\Delta_rG°_{298}$(6b) is −16.3, −11.1, and −10.4 kJ/mol. Similarly, we have the reactions for acetic acid

$$2DEE{:}BF_3 + EOX + (AcA)_2 \rightarrow DEE{:}BF_3 + DEE + bteox + (AcA)_2 \quad (7a)$$

$$2DEE{:}BF_3 + EOX + (AcA)_2 \rightarrow 2DEE + EOX + 2btaa \quad (7b)$$

obtaining a $\Delta_rG°_{298}$(7a) of 7.0, 10.5, and 10.5 kJ/mol vs $\Delta_rG°_{298}$(7b) of −3.4, 6.0, and 24.9 kJ/mol. Only for the MP2/6-311++G(3df,2pd) calculations is the result for (7b) less favorable than for (7a), a result one can pin down on the smaller stability of btaa at this level of calculation.

The situation would be different, of course, if the nucleophile had the possibility of dissociating to the conjugate base, but this is not the case in a solvent like CH_2Cl_2, which is frequently used for these reactions. The way we interpret the results we showed in this paper is that BF_3 actually prepares the nucleophilic complex in such a way that the proton from the attacking methanol or acetic acid is transferred either to the second monomer or to BF_3, so that it is available later to be transferred back, this time to the oxygen of the opened epoxide. This mechanism does not rule out that another BF_3 molecule could be simultaneously helping the reaction by combining with the oxygen of the epoxide as soon as it is polar enough due to the progress of the reaction. Work in this direction is presently being performed in our laboratory.

Conclusions

The dimers and trimers of BF_3 with several small molecules (dimethyl ether, diethyl ether, oxirane, methanol, and acetic acid) have been studied theoretically, using density functional methods and second-order perturbation theory. Most of these complexes have been fully characterized for the first time, and all of them were calculated at better levels than previously done. The comparison of theoretical and experimental data, when the latter were available, showed a satisfactory agreement, lending support to the assumption that the calculations are reasonably accurate even in those cases for which no experiments are available. The energetics of the complexation with BF_3 has been determined in all cases, and it was shown that the stability of the complexes in terms of enthalpies of complexation at 298.15 K follow the sequence $(AcA)_2{:}BF_3 > (Met)_2{:}BF_3 > (AcA)_2 > AcA{:}BF_3 > DEE{:}BF_3 > DME{:}BF_3 > Met{:}BF_3 > EOX{:}BF_3 > (Met)_2$ although the MP2 method predicts the $AcA{:}BF_3$ complex to be less stable (roughly the same as $Met{:}BF_3$). The stability of these complexes has been discussed in the context of epoxide ring opening in nonprotogenic solvents. It is suggested that for species of about the same complexity the catalyst tends to bind preferentially to the nucleophile, not to the epoxide as rules the conventional mechanism in organic chemistry. Studies are underway to verify this hypothesis in actual laboratory cases.

Acknowledgment. This work has been partially funded by Pedeciba-Uruguay. This work was done in partial fulfillment of the Ph.D. requirements of P.S. The contents of this publication do not necessarily reflect the views or policies of the DHHS, nor does mention of trade names, commercial products, or organizations imply endorsement by the U.S. Government.

References and Notes

(1) See: for instance, (a) Blackett, B. N.; Coxon, J. M.; Hartshorn, M. P.; Richards, K. E. *J. Am. Chem. Soc.* **1970**, *92*, 2574. (b) Coxon, J. M.; Thorpe, A. J.; Smith, W. B. *J. Org. Chem.* **1999**, *64*, 9575. (c) Coxon, J. M.; Thorpe, A. J. *J. Org. Chem.* **2000**, *65*, 8421 and references therein.

(2) Saenz, P.; Cachau, R. E.; Seoane, G.; Ventura, O. N., unpublished.

(3) Brown, H. C.; Adams, R. M. *J. Am. Chem. Soc.* **1942**, *64*, 2557.

(4) Laubengayer, A. W.; Finlay, G. R. *J. Am. Chem. Soc.* **1943**, *65*, 884.

(5) Bauer, S. H.; Finlay, G. R.; Laubengayer, A. N. *J. Am. Chem. Soc.* **1943**, *65*, 889.

(6) Bauer, S. H.; Finlay, G. R.; Laubengayer, A. N. *J. Am. Chem. Soc.* **1945**, *67*, 339.

(7) Iijima, K.; Yamada, T.; Shibata, S. *J. Mol. Struct.* **1981**, *77*, 271.

(8) McLaughlin, D. E.; Tamres, M. *J. Am. Chem. Soc.* **1960**, *82*, 5618.

(9) Greenwood, N. N.; Martin, R. L.; Emeleus, H. J. *J. Chem. Soc.* **1950**, 3030

(10) Grimley, J.; Holliday, A. K. *J. Chem. Soc.* **1954**, 1215.

(11) McLaughlin, D. E.; Tamres, M.; Searles, S., Jr. *J. Am. Chem. Soc.* **1960**, *82*, 5621.

(12) Maria, P.-Ch.; Gal, J.-F. *J. Phys. Chem.* **1985**, *89*, 1296.

(13) Jonas, V.; Frenking, G.; Reetz, M. T. *J. Am. Chem. Soc.* **1994**, *116*, 8741.

(14) Rauk, A.; Hunt, I. R.; Keay, B. A. *J. Org. Chem.* **1994**, *59*, 6808.

(15) Nxumalo, L. M.; Ford, T. A. *J. Mol. Struct.: THEOCHEM* **1996**, *369*, 115.

(16) Ring, S.; Eisenhardt, C. G.; Baumgärtel, H. *Chem. Phys. Lett.* **1997**, *280*, 251.

(17) Rowsell, B. D.; Gillespie, F. J.; Heard, G. L. *Inorg. Chem.* **1999**, *38*, 4659.

(18) Fărcaşiu, D.; Lukinskas, P.; Ghenciu, A.; Martin, R. *J. Mol. Catal. A* **1999**, *137*, 213.

(19) Derouault, J.; Dziembowska, T.; Forel, M.-T. *Spectrochim. Acta, Part A* **1979**, *35*, 773.

(20) Taillandier, M.; Tochon, J.; Taillandier, E. *J. Mol. Struct.* **1971**, *10*, 471.

(21) Haubein, N. C.; Broadbeldt, L. J.; Mozeleski, E. J.; Schlosberg, R. H.; Cook, R. A.; Mehnert, C. P.; Fărcaşiu, D. *Catal. Lett.* **2002**, *80*, 139.

(22) Haubein, N. C.; Broadbeldt, L. J.; Schlosberg, R. H. *Ind. Eng. Chem. Res.* **2004**, *43*, 18.

(23) Servis, K. L.; Jao, L. *J. Phys. Chem.* **1972**, *76*, 329.

(24) (a) Hehre, W. J.; Radom, L.; Schleyer, P. v. R.; Pople, J. A. *Ab Initio Molecular Orbital Theory*; Wiley: New York, 1986. (b) Jensen, F. *Introduction to Computational Chemistry*; Wiley: Chichester, West Sussex, England, 1999. (c) Foresman, J. B.; Frisch, Æ. *Exploring Chemistry with Electronic Structure Methods*, 2nd ed.; Gaussian, Inc.: Pittsburgh, PA, 1996.

(25) (a) Parr, R. G.; Yang, W. *Density Functional Theory of Atoms and Molecules*; Oxford Science Publications: Oxford, 1989. (b) *Chemical Applications of Density Functional Theory*; Laird, B. B., Ross, R. B., Ziegler, T. Eds.; ACS Symp. Series 629; American Chemical Society: Washington, DC, 1996. (c) *Density Functional Methods in Chemistry and Materials Science;* Springborg, M., Ed.; Wiley: New York, 1997. (d) Burke, K.; Perdew, J. P.; Levy, M. In *Modern Density Functional Theory: A Tool for Chemistry*, Seminario, J. M.; Politzer, P., Eds.; Elsevier: Amsterdam, 1994. (e) Lee, T. J.; Scuseria, G. E. In *Quantum Mechanical Electronic Structure Calculations with Chemical Accuracy*; Langhoff, S. R., Ed.; Kluwer: Dordrecht, Holland 1995; p 47.

(26) (a) Møller, C.; Plesset, M. S. *Phys. Rev.* **1934**, *46*, 618. (b) Head-Gordon, M.; Pople, J. A.; Frisch, M. J. *Chem. Phys. Lett.* **1988**, *153*, 503. (c) Frisch, M. J.; Head−Gordon, M.; Pople, J. A. *Chem. Phys. Lett.* **1990**, *166*, 275. (d) Frisch, M. J.; Head−Gordon, M.; Pople, J. A. *Chem. Phys. Lett.* **1990**, *166*, 281. (e) Head-Gordon, M.; Head−Gordon, T. *Chem. Phys. Lett.* **1994**, *220*, 122. (f) Saebo, S.; Almlöf, J. *Chem. Phys. Lett.* **1989,** *154*, 83.

(27) Perdew, J. P.; Burke, K.; Ernzerhof, M. *Phys. Rev. Lett.* **1996**, *77*, 3865. Perdew, J. P.; Burke, K.; Ernzerhof, M. *Phys. Rev. Lett.* **1997**, *78*, 1396.

(28) (a) Becke, A. D. *J. Chem. Phys.* **1993**, *98*, 5648. (b) Becke, A. D. *Phys. Rev. A* **1998**, *38*, 3098. (c) Lee, C.; Yang, W.; Parr, R. G. *Phys. Rev. B* **1998**, *37*, 785. (d) Miehlich, B.; Savin, A.; Stoll, H.; Preuss, H. *Chem. Phys. Lett.* **1989**, *157*, 200.

(29) (a) Carpenter, J. E.; Weinhold, F. *J. Mol. Struct: THEOCHEM* **1988**, *169*, 41. (b) J. E. Carpenter. Ph.D. Thesis, University of Wisconsin, Madison, WI, 1987. (c) Foster, J. P.; Weinhold, F. *J. Am. Chem.* Soc. **1980**, *102*, 7211. (d) Reed, A. E.; Weinhold, F. *J. Chem. Phys.* **1983**, *78*, 4066. (e) Reed, A. E.; Weinhold, F. *J. Chem. Phys.* **1983**, 1736. (f) Reed, A. E.; Weinstock, R. B.; Weinhold, F. *J. Chem. Phys.* **1985**, *83*, 735. (g) Reed, A. E.; Curtiss, L. A.; Weinhold, F. *Chem. Rev.* **1988**, *88*, 899.

(30) (a) Simon, S.; Duran, M.; Dannenberg, J. J. *J. Chem. Phys.* **1996**, *105*, 11024. (b) Boys, S. F.; Bernardi, F. *Mol. Phys.* **1970**, *19*, 553.
(31) Frisch, M. J.; Trucks, G. W.; Schlegel, H. B.; Scuseria, G. E.; Robb, M. A.; Cheeseman, J. R.; Montgomery, J. A., Jr.; Vreven, T.; Kudin, K. N.; Burant, J. C.; Millam, J. M.; Iyengar, S. S.; Tomasi, J.; Barone, V.; Mennucci, B.; Cossi, M.; Scalmani, G.; Rega, N.; Petersson, G. A.; Nakatsuji, H.; Hada, M.; Ehara, M.; Toyota, K.; Fukuda, R.; Hasegawa, J.; Ishida, M.; Nakajima, T.; Honda, Y.; Kitao, O.; Nakai, H.; Klene, M.; Li, X.; Knox, J. E.; Hratchian, H. P.; Cross, J. B.; Bakken, V.; Adamo, C.; Jaramillo, J.; Gomperts, R.; Stratmann, R. E.; Yazyev, O.; Austin, A. J.; Cammi, R.; Pomelli, C.; Ochterski, J. W.; Ayala, P. Y.; Morokuma, K.; Voth, G. A.; Salvador, P.; Dannenberg, J. J.; Zakrzewski, V. G.; Dapprich, S.; Daniels, A. D.; Strain, M. C.; Farkas, O.; Malick, D. K.; Rabuck, A. D.; Raghavachari, K.; Foresman, J. B.; Ortiz, J. V.; Cui, Q.; Baboul, A. G.; Clifford, S.; Cioslowski, J.; Stefanov, B. B.; Liu, G.; Liashenko, A.; Piskorz, P.; Komaromi, I.; Martin, R. L.; Fox, D. J.; Keith, T.; Al-Laham, M. A.; Peng, C. Y.; Nanayakkara, A.; Challacombe, M.; Gill, P. M. W.; Johnson, B.; Chen, W.; Wong, M. W.; Gonzalez, C.; Pople, J. A. *Gaussian 03*, revision B.04; Gaussian, Inc.: Wallingford, CT, 2004.
(32) Corey, E. J.; Rohde, J. J.; Fischer, A.; Azimioara, M. D. *Tetrahedron Lett.* **1997**, *38*, 33.
(33) Güizado-Rodríguez, M.; Ariza-Castolo, A.; Merino, G.; Vela, A.; Noth, H.; Bakhmutov, V. I.; Contreras, R. *J. Am. Chem. Soc.* **2001**, *123*, 9144.
(34) Nxumalo, L. M.; Ford, T. A. *J. Mol. Struct.* **2003**, *656*, 303.
(35) Nxumalo, L. M.; Ford, T. A. *Proc. SPIE-Int. Soc. Opt. Eng.*, 9th International Conference on Fourier Transform Spectroscopy; Bertie, J. E., Wieser, H., Eds., **1993**, *2089*, 200.
(36) Nxumalo, L. M.; Ford, T. A. *Mikrochim. Acta [Suppl.]* **1997**, *14*, 383.
(37) O'Neill, F. M. M.; Yeo, G. A.; Ford, T. A. *J. Mol. Struct.* **1988**, *173*, 337.
(38) Nxumalo, L. M.; Ford, T. A. *Vib. Spectrosc.* **1994**, *6*, 333.
(39) Hunt, R. L.; Ault, B. S. *Spectrosc.: Int. J.* **1982**, *1*, 45.
(40) Shibata, S.; Iijima, K. *Chem. Lett.* **1977**, 29.
(41) Begun, G. M.; Fletcher, W. H.; Palko, A. A. *Spectrochim. Acta* **1962**, *18*, 655.
(42) Taillandier, E.; Taillandier, M. *Compt. Rend.* **1962**, *257*, 1522.
(43) Lascombe, J.; Le Calvé, J.; Forel, M.-T. *Compt. Rend.* **1964**, *258*, 5611.
(44) Hirota, F.; Koyama, Y.; Shibata, S. *J. Mol. Struct.* **1981**, *70*, 305.
(45) Hargittai, M.; Hargittai, I. *Int. J. Quantum Chem.* **1992**, *44*, 1057.
(46) (a) Diehl, P. *Helv. Phys. Acta* **1958**, *31*, 686. (b) Diehl, P.; Ogg, R. A. *Nature* **1957**, *180*, 1114.
(47) Paasivirta, J.; Brownstein, S. *J. Am. Chem. Soc.* **1965**, *87*, 3593.
(48) Coussan, S.; Bouteiller, Y.; Loutellier, A.; Perchard, J. P.; Racine, S.; Peremans, A.; Zheng, W. Q.; Tadjeddine, A. *Chem. Phys.* **1997**, *219*, 221, and references therein.
(49) Masella, M.; Flament, J. P. *J. Chem. Phys.* **1998**, *108*, 7141.
(50) Tsuzuki, S.; Uchimaru, T.; Matsumura, K.; Mikami, M.; Tanabe, K. *J. Chem. Phys.* **1999**, *110*, 11906.
(51) Tsuzuki, S.; Lüthi, H. P. *J. Chem. Phys.* **2001**, *114*, 3949.
(52) Bakó, I.; Pálinkás, G. *J. Mol. Struct.: THEOCHEM* **2002**, *594*, 179.
(53) Koné, M.; Illien, B.; Graton, J.; Laurence, C. *J. Phys. Chem. A* **2005**, *109*, 11907.
(54) Fileti, E. E.; Canuto, S. *Int. J. Quantum Chem.* **2005**, *104*, 808.
(55) Schriver, L.; Burneau, A.; Perchard, J. P. *J. Chem. Phys.* **1982**, *77*, 4926.
(56) Mitev, V. M.; Stefanov, B.; Ivanov, L. M.; Georgiev, G. M. *J. Mol. Struct.* **1985**, *129*, 11.
(57) Schrems, O. *J. Mol. Struct.* **1986**, *141*, 451.
(58) Bakkas, N.; Loutellier, A.; Racine, A.; Perchard, J. P. *J. Chem. Phys.* **1993**, *90*, 1703.
(59) Lovas, F. J.; Hartwig, H. *J. Mol. Spectrosc.* **1997**, *185*, 98.
(60) Coussan, S.; Loutellier, A.; Perchard, J. P.; Racine, S.; Peremans, A.; Tadjeddine, A.; Zheng, W. Q. *Chem. Phys.* **1997**, *223*, 279.
(61) Perchard, J. P.; Mielke, Z. *Chem. Phys.* **2001**, *264*, 221.
(62) Barnes, A. J.; Hallam, H. E. *Trans. Faraday Soc.* **1970**, *66*, 1920.
(63) Huisken, F.; Kulcke, A.; Lausch, C.; Lisy, J. M. *J. Chem. Phys.* **1991**, *95*, 3924.
(64) Chocholoušová, J.; Vacek, J.; Hobza, P. *J. Phys. Chem. A* **2003**, *107*, 3086.
(65) Jones, R. E.; Templeton, D. H. *Acta Crystallogr.* **1958**, *11*, 484.
(66) Nakabayashi, T.; Kosugi, K.; Nishi, N. *J. Phys. Chem. A* **1999**, *103*, 10851.
(67) Branchadell, V.; Oliva, A. *J. Am. Chem. Soc.* **1991**, *113*, 4132.
(68) Reetz, M. T.; Hüllmann, M.; Massa, W.; Berger, S.; Rademacher, P.; Heymanns, P. *J. Am. Chem. Soc.* **1986**, *108*, 2405.
(69) Gung, B. W.; Wolf, M. A. *J. Org. Chem.* **1992**, *57*, 1370.
(70) Feng, Y.; Lu, L.; Zhao, S.-W.; Wang, J.-T.; Guo, Q.-X. *J. Phys. Chem. A* **2004**, *108*, 9196.
(71) Kieninger, M.; Ventura, O. N. To be published.
(72) Rutenberg, A. C.; Palko, A. A.; Drury, J. S. *J. Am. Chem. Soc.* **1963**, *85*, 2702.
(73) VanDyke, C. H.; MacDiarmid, A. G. *J. Phys. Chem.* **1963**, *67*, 1930.
(74) Gore, E.; Danyluk, S. S. *J. Phys. Chem.* **1965**, *69*, 89.
(75) Begun, G. M.; Palko, A. A. *J. Chem. Phys.* **1963**, *38*, 2112.